Environmental Changes during the Cretaceous-Paleogene Mass Extinction and Paleocene-Eocene Thermal Maximum: Implications for the Anthropocene

Gerta Keller[1], Paula Mateo[1], Jahnavi Punekar[2], Hassan Khozyem[3], Brian Gertsch[4], Jorge Spangenberg[5], André Bitchong[6] and Thierry Adatte[4]

[1]Department of Geosciences, Princeton University, Princeton, NJ 08544, USA

gkeller@exchange.Princeton.EDU, mmateo@princeton.edu

[2]Indian Institute of Technology Bombay, Mumbai 400076, India jpunekar@iitb.ac.in

[3]Department of Geology, Faculty of Sciences, Aswan University, Aswan, Egypt

hkhozyem@gmail.com

[4]Institute of Earth Sciences (ISTE), University of Lausanne, 1015 Lausanne, Switzerland

thierry.adatte@unil.ch, briangertsch1@gmail.com

[5]Institute of Earth Surface Dynamics (IDYST), University of Lausanne, Switzerland, 1015 Lausanne, Switzerland jorge.spangenberg@unil.ch

[6]Department of Earth Sciences, Faculty of Science, University of Yaounde 1, P.O. Box 812 Yaounde, Cameroon; Department of Petroleum and Gas Exploration, Institute of Mines and Petroleum Industries, University of Maroua, P.O. Box 08 Kaele, Cameroon

andrembabi@gmail.com

ABSTRACT

The Cretaceous-Paleogene boundary (KPB) mass extinction (~66.02 Ma) and the Paleocene-Eocene Thermal Maximum (PETM) (~55.8 Ma) are two remarkable climatic

and faunal events in Earth's history that have implications for the current Anthropocene global warming and rapid diversity loss. Here we evaluate these two events at the stratotype localities in Tunisia and Egypt based on climate warming and environmental responses recorded in faunal and geochemical proxies. The KPB mass extinction is commonly attributed to the Chicxulub impact, but Deccan volcanism appears as a major culprit. New mercury analysis reveals that major Deccan eruptions accelerated during the last 10 ky and reached the tipping point leading up to the mass extinction. During the PETM, climate warmed rapidly by ~5 ºC, which is mainly attributed to methane degassing from seafloor sediments during global warming linked to the North Atlantic Igneous Province (NAIP). Biological effects were transient, marked by temporary absence of most planktic foraminifera due to ocean acidification followed by the return of the pre-PETM fauna and diversification. In contrast, the current rapid rise in atmospheric CO_2 and climate warming are magnitudes faster than at the KPB or PETM events leading to predictions of a PETM-like response as best case scenario and rapidly approaching sixth mass extinction as worst-case scenario.

1. INTRODUCTION

One of the greatest challenges to our planet is the looming Anthropocene mass extinction commonly attributed to human activity as the dominant influence on rapid climate warming and changing environments as a result of fossil fuel burning (IPCC 5th Assessment Report, 2013). This climate warming is commonly compared with the rapid short-term ~5 ºC warming known as the Paleocene-Eocene Thermal Maximum (PETM)

47 ~55.8 Ma. However, the PETM led to opposite results: major diversification in marine
48 and terrestrial life and significant species extinctions only in deep-water benthic
49 foraminifera. A better understanding of the impending Anthropocene catastrophe can be
50 gained from the rapid warming and mass extinction culminating at the Cretaceous-
51 Paleogene boundary (KPB also known as KPgB or KTB). In this study we examine both
52 the PETM and KPB events to gain insights into potential Anthropocene scenarios.

53 The PETM event (55.8 ± 0.2 Ma) lasted ~170 ky and is commonly attributed to
54 North Atlantic Igneous Province (NAIP) volcanism and methane degassing of seafloor
55 sediments (e.g., Dickens et al., 1995; Dickens, 2000; Westerhold et al., 2009; Charles et
56 al., 2011; Wieczorek et al., 2013; Gutjahr et al., 2017). The resulting global negative $\delta^{13}C$
57 excursion of 2-6 ‰ and rapid warming of 4.5-5 °C from tropical to high latitudes was
58 accompanied by ocean acidification and shoaling of the carbonate compensation depth
59 (CCD) by ~2000 m (e.g., Kennett and Stott, 1991; Sluijs et al., 2006; Zachos et al., 2003,
60 2005, 2006; Weijers et al., 2007; McInnery and Wing, 2011; Coccioni et al., 2012;
61 Gutjahr et al., 2017). In the marine realm planktic foraminifera and calcareous
62 nannoplankton, which form the essential food chain in the oceans, temporarily
63 disappeared but returned and diversified after the PETM (Lu and Keller, 1993, 1995a, b;
64 Kelly et al., 1996, 1998; Luciani et al., 2007, 2016). Only benthic foraminifera suffered
65 significant extinctions and these were restricted to bathyal depths where an estimated 37
66 % species went extinct (Alegret and Ortiz, 2006). No other groups in marine or terrestrial
67 realms suffered significant extinctions. On land tropical and subtropical forests spread
68 into higher latitudes during the PETM (Sluijs et al., 2006) and most animals reduced in

size and abundance (Smith et al., 2009). Shortly after the PETM mammals migrated, thrived and diversified (Smith et al., 2009).

The KPB mass extinction (66.02 Ma) was marked by a negative 2-3 ‰ $\delta^{13}C$ shift in surface but not deep waters, leading to an inverse surface-to-deep $\delta^{13}C$ gradient generally attributed to reduced primary productivity and weakening of the marine biological carbon pump (e.g., Zachos et al., 1989; Kump, 1991, 2003). Rapid climate warming during the last 250 ky of the Maastrichtian, prior to the KPB, and cooling during the first 500 ky of the early Paleocene are linked to Deccan volcanic eruptions (review Punekar et al., 2014) About 50-75 % of all terrestrial and marine taxa went extinct. In the oceans, extinctions affected the base of the food chain most severely causing major extinctions in calcareous nannoplankton and near total extinction (99 %) of marine planktic foraminifera (e.g., Keller, 1988a, 2001; MacLeod et al., 1997; Molina et al., 1998; Keller et al., 2002; Luciani, 2002), but no significant extinctions in benthic foraminifera (review in Culver, 2003). The extinction of non-avian dinosaurs is the most famous example of the KPB mass extinction on land while many mammals survived undergoing an explosive radiation during the Paleogene (review in Feduccia, 2014; Wilson, 2014). Macrofloral diversity also decreased during the late Maastrichtian warming and across the mass extinction horizon (e.g., Wilf et al., 2003; Wilf and Johnson, 2004).

Both PETM and KPB events thus recorded extreme and rapid climate changes but with nearly opposite effects on marine and terrestrial life – rapid evolutionary diversification following the PETM event with extinctions restricted to deep water benthic foraminifera but near total mass extinction in planktic foraminifera at the KPB.

Understanding when rapid climate change furthers evolutionary diversification and when it leads to extinctions is critical to assessing the risk of current climate warming for marine and terrestrial populations including humans in the coming decades. This study explores the potential reasons for the differing biotic responses associated with rapid climate warming during the PETM and KPB events and compares these with the current rapid climate warming and biotic response of the Anthropocene. We hypothesize that the biotic response mainly depends on the rate and tempo of greenhouse gas emissions into the atmosphere and that extinctions are inevitable once the tipping point or critical threshold is reached, which marks the onset of irreversible climate change from which even small perturbations can result in runaway effects.

For this study we chose the globally recognized most complete sections for the KPB and PETM events. For the KPB these are the Global Stratotype Section and Point (GSSP) at El Kef and the auxiliary stratotype at Elles (Molina et al., 2009) 56 km southeast of the city of El Kef, Tunisia, and for the PETM, the global GSSP at the Dababiya quarry in Egypt (Figs. 1, 2). We focus on four topics: 1) planktic and benthic species population changes in foraminifera, the groups most strongly affected by both events; 2) evidence linking mass extinctions and faunal turnovers to climate change and ocean acidification; 3) evidence linking these faunal events directly to volcanism; and 4) comparison of KPB and PETM with the Anthropocene and potential sixth mass extinction. Analyses are based on benthic and planktic foraminifera, carbon and oxygen stable isotopes, mineralogy, and mercury (Hg) anomalies. (A description of methods, materials and locations and of the environmental proxies is given in Supplementary Materials S1; data tables are given in Supplementary Materials S2.)

2. KPB MASS EXTINCTON: EL KEF AND ELLES

2.1. KPB-Defining Criteria

The KPB is one of the easiest period boundaries to identify, whether based on lithological changes in the field (Fig. 3), geochemical analysis in the laboratory, or fossil content. The El Kef section was officially designated in 1989 as the Global Stratotype Section and Point (GSSP) and Elles (discovered in the late 1990s) designated as auxiliary stratotype (Molina et al., 2009). The five KPB defining and marker criteria are: (1) mass extinction in planktic foraminifera, (2) evolution of first Danian species, (3) KPB clay and red layer, (4) iridium (Ir) anomaly and (5) $\delta^{13}C$ negative shift. These KPB criteria have proven globally applicable and independently verifiable in over 300 KPB sequences worldwide (Cowie et al., 1989; Keller et al., 1995; Remane et al., 1999). Since planktic foraminifera are the only marine microfossil group that suffered near total extinction, they have remained the most reliable KPB-defining criteria. All other KPB markers, such as the clay and red layers, Ir anomaly and $\delta^{13}C$ shift, are not unique signals in the geological record and therefore cannot define the KPB in the absence of unique biomarkers (review in Keller, 2011).

However, proponents of the Chicxulub impact as sole cause for the mass extinction eliminated the five KPB identifying criteria in favor of just the "*Ir anomaly associated with a major extinction horizon*" (Gradstein et al., 2004, ICS website on GSSPs). Based on these two criteria and the assumption that the Ir anomaly is the result of the Chicxulub impact, Molina et al. (2006, p. 263) concluded that "*in this way the KPB*

is marked exactly by the moment of the meteorite impact" and that "*This definition solves problems of correlation in the Yucatan peninsula (Mexico) and its surroundings*." Far from solving "problems of correlation", this new definition has only introduced circular reasoning to support the hypothesis that the Chicxulub impact is precisely KPB in age, thus ignoring contrary evidence (Keller, 2011, Supplementary Materials S3). Fortunately, the El Kef and Elles KPB sections remain identified by the original five criteria that are the most reliable KPB markers.

2.2. Biostratigraphy: Planktic Foraminifera

Zone definitions are based on Keller et al. (1995, 2002) and include: zone CF2 (last appearance (LA) of *Gansserina gansseri* near the base of magnetochron C29r to first appearance (FA) of *Plummerita hantkeninoides*), zone CF1 (range of *Plummerita hantkeninoides,* extinct at the KPB), zone P0 (from the KPB to FA of *Parvularugoglobigerina eugubina*), zone P1a(1) (FA of *P. eugubina* to FAs of *Parasubbotina pseudobulloides* and/or *Subbotina triloculinoides*), and zone P1a(2) (LAs of *P. eugubina* and *P. longiapertura*) correlative with the top of magnetochron C29r (Fig. 4). Thus, zones CF2 through P1a(2) correlate with magnetochron C29r (Li and Keller, 1998; Pardo et al., 1996). The time interval presented in this study for El Kef spans from the latest Maastrichtian zone CF1 through the early Danian zones P0, P1a(1), P1a(2) and lower part of P1b and for Elles from the upper part of zone CF1 to zone P1a(1)..

Recent U-Pb zircon dating of Deccan Traps yielded a duration of ~750 ky for C29r (Schoene et al., 2015) with 200 ky equivalent to zone CF1 below the KPB and 500 ky equivalent to P0, P1a(1) and P1a(2) above the KPB. The late Maastrichtian intervals

used in this study at El Kef and Elles span the last ~68 ky and 70 ky below the KPB and first ~500 ky and ~150 ky of the early Danian, respectively, plus an unknown age interval of zone P1b in C29n (Fig. 4).

2.3. Extinctions and Survivals

The mass extinction at El Kef is shown in Figure 4 based on species ranges and morphologies of the different planktic foraminiferal groups. The largest most specialized and highly ornamented taxa, known as K-strategists (Fig. 4 #1-10), generally lived below the surface in tropical and subtropical waters, utilized specialized food sources, had few offspring and lived longer (Begon et al., 1996, 1998). They suffered reduced population abundances and species dwarfing during the late Maastrichtian climate warming linked to Deccan volcanism in C29r, zones CF1-CF2 (Li and Keller, 1998; Olsson et al., 2001; Abramovich et al., 2003, 2010; Keller and Abramovich, 2009; Punekar et al., 2014; Thibault et al., 2016; Thibault and Husson, 2016).

Quantitative species abundances at El Kef show that during this global warming complex larger specialized species decreased in abundance and diversity (Fig. 5) as also observed at Elles and worldwide (Abramovich and Keller, 2002; Punekar et al., 2014; Keller et al., 2016). Among this group, the robust globotruncanids (16 species) are generally rare with combined abundance of 6-13 %, which demonstrates the severe toll climate warming and related stresses (e.g., ocean acidification, high nutrient influx from Deccan volcanism and terrestrial runoff due to increased humidity) exerted on marine plankton leaving them prone to extinction.

A small group of species (about 1/3 of planktic foraminiferal assemblages) survived relatively well during the pre-KPB C29r climate warming (zone CF1, Figs. 4, 5). These were relatively small species with simple biserial and trochospiral morphologies, with little shell ornamentation. They were ecologically more tolerant, r-strategists that thrived in varied environments from low to high latitudes, utilized diverse food sources, had short life spans and reproduced rapidly with many offspring (review in Keller and Abramovich, 2009). This group had high survival potential but just one species survived long-term – the disaster opportunist *Guembelitria cretacea*.

There is general agreement that between 8-16 smaller species survived for about 50-150 ky into the early Danian (Figs. 4, 5) but survivorship is difficult to ascertain for most species because reworked Cretaceous species are common above the KPB. This is mainly due to the early Danian global cooling, lower sea level and erosion that frequently resulted in hiatuses eroding the underlying KPB interval and latest Maastrichtian particularly in shallow water environments (Keller et al., 2013, 2016; Mateo et al., 2017). Clues to survivorship include consistent presence in Danian sediments, good preservation, generally dwarfed specimens and Danian isotope values. Only *Heterohelix globulosa, H. planata, Paraspiroplecta navarroensis, Pseudoguembelina costulata, Guembelitria cretacea, Hedbergella monmouthensis, H. holmdelensis, Globigerinelloides asper and G. yaucoensis* are proven mass extinction survivors to date (e.g., Barrera and Keller, 1990; Pardo and Keller, 2008; Ashckenazi-Polivoda et al., 2011). Other species are also consistently present well into the early Danian but have yet to be conclusively determined as survivors (e.g., *Pseudoguembelina costellifera, P. kempensis, Globigerinelloides subcarinatus*; Figs. 4-6).

Among the survivors, four biserial species (*P. costulata*, *H. globulosa*, *H. planata*, *P. navarroensis*), at least three trochospiral species (*Hedbergella monmouthensis, H. holmdelensis, Globigerinelloides yaucoensis*), and one triserial species (*G. cretacea*), are known to tolerate low oxygen conditions. These dominate late Maastrichtian assemblages and range well into the early Danian with reduced to sporadic presence (Figs. 4-6) (Pardo and Keller, 2008; Ashckenazi-Polivoda et al., 2011). But they also suffered beginning in the latest Maastrichtian (upper zone CF1) and into the early Danian as evident by species dwarfing, deformed chambers and reduced population abundances (Fig. 6) (review in Keller and Abramovich, 2009).

The KPB mass extinction has just one long-term survivor, *G. cretacea,* which is known as a disaster opportunist. This species thrived during maximum stress conditions and dominated faunal assemblages of the latest Maastrichtian and early Danian (>90 %) at El Kef and Elles (Figs. 5, 6) (Pardo and Keller, 2008; Punekar et al., 2014). *Guembelitria cretacea* was the smallest planktic foraminifer (63-100 μm) and responded to high-stress conditions by dwarfing (size reduction to 38-63 μm), irregular deformed chambers (Coccioni and Luciani, 2006), and less frequently gigantism (Keller, 2014). During optimal environmental conditions, this disaster opportunist disappeared from open marine assemblages but survived in high-stress near-shore refugia.

2.4. Species Dwarfing

Species dwarfing, also known as the Lilliput effect, marks morphologic and intraspecies size reductions in response to environmental stresses commonly associated with, but not restricted to, the aftermath of mass extinctions (Keller and Abramovich,

2009). In addition to planktic foraminifera across the KPB mass extinction, the Lilliput effect has been observed in many groups, including ostracods, mollusks and bivalves, of the Permo-Triassic mass extinction (Payne, 2005; Twitchett, 2007; Chu et al., 2015), shelly faunas and microbial carbonates preceding the end-Devonian mass extinction (Whalen et al., 2002; Bosetti et al., 2010), crinoids of the end-Ordovician mass extinction (Borths and Ausich, 2011) and graptolites of the upper Silurian (Urbanek, 1993). This suggests a universal biotic response to environmental stress, regardless of cause, timing or nature of organisms.

High-stress environments are associated with rapid climate change, mesotrophic or restricted basins, shallow marginal settings and volcanically active regions. For example, Large Igneous Province (LIP) volcanism is currently associated with four of the five Phanerozoic mass extinctions, whereas Hg anomalies, a proxy for volcanism, are reported from all five (da Silva et al., 2008; Grasby et al., 2013; Percival et al., 2015; Thibodeau et al., 2016; Font et al., 2016; Gong et al., 2017). Second order volcanic events (e.g., Ninetyeast Ridge and Andean volcanism) are at least in part related to the early late Maastrichtian faunal turnover (Keller, 2003; Keller et al., 2007; Mateo et al., 2017).

Among planktic foraminifera the sequence of responses to increasingly high environmental stress developed in 5 stages that form a stress continuum from optimum open marine conditions to increasingly stressful environments associated with rapid climate warming and volcanic activity leading to catastrophe (Fig. 7). The five stages of this stress continuum include: (1) elimination of large specialized species (K-strategists), (2) intraspecies dwarfing, (3) dominance of low oxygen tolerant small heterohelicids (r-

252 strategists), (4) decline of heterohelicids and (5) dominance of disaster opportunist
253 *Guembelitria* species (Keller and Abramovich, 2009).

254 This sequence of stress-induced biotic events is demonstrated at El Kef and Elles,
255 as well as in all continuous KPB sequences worldwide (Pardo and Keller, 2008; Keller
256 and Abramovich, 2009). Stages 1-2 are evident by the dramatic reduction in large K-
257 strategist species populations and dwarfing of survivors, which was first linked to global
258 warming caused by Deccan volcanism in magnetochron C29r at South Atlantic DSDP
259 Site 525A (Abramovich and Keller, 2003). Stage 3 marks the rising dominance of r-
260 strategists, followed by dwarfing in stage 4 and declining populations. Stage 5 marks
261 maximum stress resulting in decreased populations of r-strategists and dominance of the
262 disaster opportunist *Guembelitria.*

263 Figure 6 shows the effects of species dwarfing across the KPB transition based on
264 >63 μm and 38-63 μm size fractions at Elles. In the >63 μm size fraction below the KPB,
265 the same four biserial taxa dominate the assemblage as at El Kef and *Guembelitria*
266 *cretacea* is rare (Fig. 6A). After the mass extinction, *G. cretacea* dominates (>95 %) but
267 the interval between 7 cm to 80 cm above the KPB is barren in the >63 μm size fraction
268 with species abruptly reappearing above (Fig. 6A).

269 Analysis of the smaller size fraction (38-63 μm) reveals the missing fauna as
270 dwarfed due to increased stress (Fig. 6B). The most notable difference is the dominance
271 of dwarfed disaster opportunist *G. cretacea* and low oxygen tolerant *P. navarroensis* and
272 *H. planata*. Dwarfed *Guembelitria* populations up to 90 % of the total foraminiferal
273 assemblages are frequently observed below the KPB in shallow shelf to open marine and
274 in volcanically stressed environments (review in Pardo and Keller, 2008). Similar

Guembelitria blooms dominated (~90 %) after the KPB mass extinction, although they are generally not dwarfed. This suggests that environmental stress was higher before the mass extinction than in its aftermath.

2.5. Evolution and Delayed Recovery

Evolution of new species began in zone P0 immediately after the mass extinction (Fig. 8). The first new species were very small (38-63 μm), unornamented, with simple globular chamber arrangements in biserial, triserial and trochospiral morphologies (Figs. 4-6). Low diversity assemblages of 10 to 15 species with slightly larger (63-100 μm) morphologies persisted for the first 500 ky (zones P1a(1)-P1a(2)) after the mass extinction, marking a long crisis interval. Cretaceous survivor species gradually disappeared in zone P1a(1) (Fig. 8). Dwarfing, slow evolution, simple small species morphology and gradual disappearance of dwarfed survivor species during the early Danian mark continued high-stress environments dominated by the disaster opportunist *Guembelitria* and the new crisis opportunists *Parvularugoglobigerina eugubina* and *P. longiapertura* (Figs. 5, 6).

A clue to the nature of this crisis interval is seen in the negative 2-3 ‰ $\delta^{13}C$ excursion at the KPB that represents a sudden drop in primary marine productivity at the mass extinction horizon (Fig. 5). During the early Danian, planktic $\delta^{13}C$ values at El Kef and Elles remained 1-2 ‰ below benthic values for the first ~500 ky correlative with the delayed recovery in marine plankton (Keller and Lindinger, 1989; Stüben et al., 2003). This interval is followed by the rapid positive 2 ‰ $\delta^{13}C$ excursion at the P1a(2)/P1b zone boundary (C29r/C29n) that signals the onset of recovery coincident with the end of the

298 main phase of Deccan volcanism (Fig. 5). Thus the delayed recovery appears to be due to
299 continued volcanic eruptions. For marine plankton, the $\delta^{13}C$ recovery lead to a major re-
300 organization, including the near disappearance of the disaster opportunist *Guembelitria*
301 (Fig. 5), extinction of the dominant crisis interval taxa (*P. eugubina, P. longiapertura, P.*
302 *extensa),* dominance of *Praemurica taurica* and small biserial low oxygen tolerant
303 species (*Chiloguembelina morsei, Woodringina hornerstownensis, W. claytonensis*),
304 increased diversity and gradual appearance of larger morphotypes particularly in zone
305 P1c (Fig. 8).
306
307 **2.6. Benthic Foraminifera**
308 There is no mass extinction in benthic foraminifera across the KPB globally but
309 they suffered a severe and prolonged faunal turnover (Fig. 9). At El Kef, 42 % (21
310 species) of 50 calcareous benthic species identified disappeared at the KPB and remained
311 absent through the early Danian zone P1a-P1b interval analyzed (>500 ky) (Keller
312 1988b). During the early Danian P0-P1a high-stress interval, 16 % (8 species)
313 temporarily disappeared, 30 % (15 species) ranged through with *Anomalinoides acutus*
314 dominant in the high-stress P1a interval and 12 % (6 species) appeared in the early
315 Danian. Correlative with this faunal turnover is the drop in $CaCO_3$ from ~50 % (pre-
316 KPB) to <10 % (post-KPB) in the sediments, high terrestrial organic influx (due to
317 enhanced weathering) and low oxygen in the water column and seafloor sediments
318 (Keller and Lindinger, 1989). These high nutrient conditions favored epifaunal
319 assemblages dominated by *A. acutus* scavenging food on the seafloor. Infaunal
320 assemblages largely disappeared returning with increased oxygen in sediments in zone

P1b (Fig. 9). Speijer and Van der Zwaan (1996) also analyzed El Kef benthic foraminifera. Their faunal turnover results slightly differ from Keller (1988b) with the main difference being the larger number of disappearing and temporarily absent species, which is largely due to their inclusion of agglutinated and non-specified genera groupings.

How representative is the El Kef benthic faunal turnover pattern on a global basis? Culver (2003, p. 214) reviewed published reports across latitudes and palaeodepths and concluded: "*if the percentage data are taken at face value and averaged for shallow, intermediate and deep water, the results come out as follows: shallow, 40 % disappear; intermediate, 35 % maximum, 29 % minimum disappear; deep, 29 % maximum, 19 % minimum disappear*." Note that "disappear" means that most or all of these taxa returned after the stress event in the aftermath of the KPB mass extinction. Although these data are incomplete and percentage values may have large errors, a major environmental change is evident on the seafloor across latitudes and palaeodepths but no mass extinction is recorded.

3. ENVIRONMENTAL PROXIES: KPB

During the late Maastrichtian, rapid and extreme climate warming, interrupted by short cool events, began in the lower half of zone CF2, coincident with the onset of major Deccan volcanic eruptions near the base of C29r about 350 ky prior to the mass extinction (Li and Keller, 1998; Punekar et al., 2014; Thibault et al., 2016). Figure 10 shows climate changes ($\delta^{18}O$) and Hg anomalies (proxy for Deccan volcanism) during

344 the last 70 ky of the Maastrichtian leading up to the mass extinction at Elles. No
345 temperatures have been calculated from this $\delta^{18}O$ data because diagenetic alteration of
346 foraminiferal shell calcite shifts values negative though temperature trends are preserved
347 (see Supplementary Materials S4). Hg in sediments is a byproduct of explosive
348 volcanism and has a residence time of 1-2 years in the atmosphere during which it is
349 distributed by winds worldwide before fallout and accumulation in sediments (Grasby et
350 al., 2013; Thibodeau and Bergquist, 2017). Since Hg is commonly concentrated in
351 organic carbon, it is typically normalized and shown as the ratio of Hg to total organic
352 carbon (Hg/TOC).

353 The Elles $\delta^{18}O$ record indicates a relatively cool climate from 70-40 ky pre-KPB
354 during a volcanically quiet period (Fig. 10). About 40 ky pre-KPB, surface water rapidly
355 warmed coincident with major Deccan eruptions but warming in bottom waters is
356 delayed by several thousand years. During the last 10 ky pre-KPB, climate remained
357 warm and Hg/TOC ratios remained high. Through this interval Hg/TOC ratios mark peak
358 volcanic activity with accelerating eruptions reaching maximum values at the KPB mass
359 extinction (2498 ppb/wt%; 1291 ppb/wt% at El Kef).

360 We interpret the Hg/TOC ratios at Elles as recording Deccan eruptions with the
361 high ratios indicating larger or more explosive eruptions. Maximum climate warming and
362 accelerating massive Deccan eruptions during the last 10 ky may mark the tipping point
363 for planktic foraminifera. From this point on, extinctions are rapid culminating at the
364 KPB. Faunal assemblages during this interval are dominated by stress-tolerant and
365 generally dwarfed survivor taxa with the disaster opportunist *G. cretacea* being the most
366 abundant (Figs. 5, 6A,B). At El Kef, faunal proxies indicate diversity loss, decreasing

P/B ratio, increasing fragmentation in planktic foraminifera due to dissolution and high abundance of dwarfed *Guembelitria* populations (Fig. 11). Similar faunal extinctions, disaster opportunists and dissolution coincident with high Hg/TOC ratios have been recorded during the last 30-50 ky pre-KPB in France, Austria and Spain and interpreted as ocean acidification (Font et al., 2016; Punekar et al., 2016).

Ocean acidification linked to Large Igneous Province (LIP) volcanism has been identified for the PETM and mass extinctions at the KPB, end-Triassic and end-Permian (Hönisch et al., 2012). CO_2 emissions into the atmosphere from LIP volcanism can severely perturb the carbon cycle. If the rate of atmospheric pCO_2 increase overtakes the buffering time/capacity of the ocean (~1000 yrs; Zeebe, 2012), seawater carbonate chemistry can be seriously altered resulting in the lowering of carbonate ion concentration ($[CO_3^{2-}]$) and the surface ocean pH (Kump et al., 2009). Ocean acidification leads to calcification crises in shelly organisms, such as nannofossils, foraminifera, bivalves, gastropods and pteropods, and has increasingly been identified as an important mechanism linking major volcanic episodes, including the PETM and KPB, with faunal turnovers and mass extinction events (Hönisch et al., 2012; Font et al., 2016; Punekar et al., 2016; Bond and Wignall, 2016).

The most characteristic KPB signals, apart from the Ir anomaly and mass extinction, are the drop in $CaCO_3$ to near 0 %, the Hg anomalies and high Hg/TOC ratios, and the 2-3 ‰ drop in $\delta^{13}C$, which is attributed to the mass extinction, loss of primary productivity and collapse of the biological carbon pump (Fig. 11). All faunal proxies indicate continued high-stress conditions through the early Danian C29r (~500 ky). The inverse surface-to-deep $\delta^{13}C$ gradient persisted for ~1 Myr into C29n and $CaCO_3$

remained low (<10 %). During these stress conditions the disaster opportunist *Guembelitria* dominated but alternated with the evolving short-ranging opportunist *P. longiapertura* (Fig. 5). The onset of recovery resulted in the extinction of the latter, near disappearance of the former, increased abundance of earlier taxa and evolution of new species. The recovery is led by a gradual return to higher productivity ($\delta^{13}C$) and increased $CaCO_3$ (>30 %) (Fig. 11). The cause for this delayed recovery has long remained an enigma. The answer appears to be continued Deccan volcanism after the mass extinction as indicated by Hg/TOC anomalies.

4. PALEOCENE-EOCENE THERMAL MAXIMUM (PETM): DABABIYA (GSSP)

The Dababiya GSSP is located on the eastern side of the upper Nile Valley and 35 km southeast of Luxor at 25º30'N, 32º31'E (Fig. 2). Sediment deposition occurred at outer shelf depth between 150-200 m (Alegret et al., 2005) in a submarine channel (Fig. 12A-C). The outcrop is fragile because it forms a precarious point jutting out at the turning point between eastern and northwestern parts of the channel and a vertical fracture runs through it. The section was sampled at 50 m to the northwest and 25 m to the east of the turning point, which partially collapsed in the spring of 2016 along the vertical fracture (Fig. 12C).

Khozyem et al. (2014, 2015) published geochemical and stratigraphic studies of the two sampled sequences. Earlier publications reported on mineralogy and geochemistry (Dupuis et al., 2003; Soliman et al., 2006; Schulte et al., 2011), and planktic and benthic foraminifera (Speijer et al., 1995; Speijer and Schmitz, 1998; Speijer

413 and Wagner, 2002; Berggren and Ouda, 2003; Alegret et al., 2005; Alegret and Ortiz,
414 2006). Here we present new quantitative data on the planktic foraminiferal response to
415 the PETM event at the section 25 m east from the GSSP cliff compared with benthic
416 foraminifera and previously published stable isotope records (Alegret and Ortiz, 2006;
417 Dupuis et al, 2003) (Fig. 12B, C).
418
419 **4.1. PEB-Defining Criteria**
420 The PEB is defined based on: (1) global $\delta^{13}C_{org}$ and $\delta^{13}C_{carb}$ isotope excursions
421 (CIE), (2) disappearance of the deep water benthic foraminifer *Stensioina beccariiformis*,
422 (3) transient occurrence of planktic foraminifera (*Acarinina africana, A. sibaiyaensis,*
423 *Morozovella allisonensis)* during the $\delta^{13}C$ excursions, (4) transient occurrence of the
424 nannofossil *Rhomboaster spp. – Discoaster araneus* assemblage and (5) acme of the
425 dinoflagellate *Apectodinium* (Aubry et al., 2007). At our Dababiya section 25 m east of
426 the GSSP cliff, these PEB defining characteristics are identified. Lithology and
427 geochemistry are discussed in Khozyem et al. (2014, 2015).
428
429 **4.2. Biostratigraphy: Planktic Foraminifera**
430 Biostratigraphy for the Dababiya section is based on high-resolution planktic
431 foraminifera and the standard biozonation scheme by Olsson et al. (1999) and Pearson et
432 al. (2006) (Fig. 13A). The sampled interval spans zones P4c, P5, E1 and E2 covering an
433 estimated time span of 2 Myr (54.5-56.5 Ma). Zone P4c marks the base of the section as
434 indicated by the last appearance (LA) of the index species *Globanomalina*
435 *pseudomenardii* and an assemblage dominated by *Igorina tadjjikistanensis, Acarinina*

436 *soldadoensis*, *Subbotina hornibrooki*, *Morozovella acuta* and *M. aequa*. The interval
437 from the extinction of *Gl. pseudomenardii* to the first appearance (FA) of *Acarinina*
438 *sibaiyaensis* defines zone P5 and the top of the Paleocene. At Dababiya, zone P5 marks
439 the onset of the PETM with a 40 % increase in species diversity (from 21 to 35 species)
440 and decreased abundance of the dominant zone P5 species correlative with a gradual
441 decrease in $\delta^{13}C_{org}$ and $\delta^{13}C_{carb}$ values culminating at the PEB (Fig. 13A).

442 Above the PEB, zone E1 spans 1 m with the basal 42 cm a barren clay devoid of
443 $CaCO_3$ marking dissolution/ocean acidification (Fig. 13A). Between 42-47 cm is a 5 cm
444 thick radiolarian-rich interval with the transient PETM fauna dominated by *A.*
445 *sibaiyaensis* and *A. africana* and FA of *A. africana* and *Morozovella allisonensis*. The 50
446 cm above mark the onset of recovery with increasing $\delta^{13}C$ values and rare foraminifera in
447 the upper 20 cm. The E1/E2 boundary is placed at the first continuous occurrence of
448 *Pseudohastingerina wilcoxensis* 1 m above the PEB coincident with the reappearance of
449 diverse assemblages that existed already during the latest Paleocene. Just four species
450 disappeared as they morphed into new species - a phenomenon known as
451 pseudoextinction. Returning species have generally larger shell sizes than before their
452 temporary disappearance, show morphological diversification and speciation (Lu and
453 Keller, 1993, 1995a, b; Lu et al., 1998; Kaiho et al., 2006; Kelly et al., 1996, 1998; Pardo
454 et al., 1999; Berggren and Ouda, 2003; Luciani et al., 2007, 2016; Khozyem et al., 2014).
455 Thus, despite major climate warming, decreased productivity and ocean acidification, the
456 PETM caused no significant species extinctions, likely due to migration into higher
457 latitudes during warming, and fostered major diversification in its aftermath.
458

4.3. Benthic Extinction and Faunal Turnover Event

Alegret et al. (2005, Alegret and Ortiz, 2006) reported a major benthic faunal turnover at the Dababiya section (Fig. 13B) but only 7 species (18 %) went extinct, 82 % were survivors that reappeared after the PETM acidification event, and 26 % new species evolved during environmental recovery. Similar observations are reported from marginal and epicontinental seas (Speijer and Schmitz, 1998; Speijer and Wagner, 2002). But in lower bathyal to abyssal environments (e.g., Alamedilla, Spain) species extinctions reached ~37 % (Alegret et al., 2009), which is in the lower estimate of the previously reported extinction ranging between 30-50 % (Thomas, 1998). Thus, significant benthic extinctions were restricted to deep-water environments and generally concentrated at the onset of the PETM event. This can be explained by the observed shoaling of the CCD by 2000 m during the PETM (Zachos et al., 2008).

5. ENVIRONMENTAL PROXIES: PEB

The PETM is marked by a global temperature increase of 5-9 °C over an interval variously estimated ~10 ky or ~30 ky and estimated loading of 2,000 Gt of isotopically light carbon to the atmosphere and oceans (Zachos et al., 2003, 2005, 2006; Sluijs et al., 2006; Weijers et al., 2007). A low correlation coefficient of $CaCO_3$ vs. $\delta^{13}C_{carb}$ (R^2 = 0.025) indicates limited diagenetic overprinting on the $\delta^{13}C_{carb}$ values but $\delta^{18}O$ data are strongly affected by diagenesis (see Supplementary Materials S4, Fig. S11).

Faunal, geochemical and volcanic proxies illustrate the high-stress conditions across the PETM (Fig. 14). At the base of the section (zone P4C), a short dissolution

482 event is marked by near-absence of planktic species, decreased $CaCO_3$ from 50 % to 40
483 % and maximum Hg/TOC ratios. In contrast, benthic species are well preserved. This
484 suggests surface ocean acidification as a result of peak volcanic emissions (NAIP).
485 Above this interval planktic and benthic species show dissolution effects with just 1/3
486 well-preserved 'good' planktic and between 20-60 % 'good' benthic foraminifera.
487 Hg/TOC ratios as well as $\delta^{13}C_{carb}$ and $\delta^{13}C_{org}$ values gradually decreased reaching
488 minimum values 20 cm below the PEB and at the PEB, respectively (Fig. 14).

489 A similar gradual $\delta^{13}C_{org}$ decrease has been reported from Alamedilla, Spain, (Lu
490 et al., 1996) and Spitsbergen, Norway, with the latter linked to North Atlantic Igneous
491 Province (NAIP) volcanism (Wieczorek et al., 2013). At Dababiya Hg/TOC ratios
492 (ppb/wt%) also link this interval to NAIP. At all three sites the isotopic records are
493 interpreted as gradually increasing ocean temperatures due to atmospheric CO_2 loading
494 linked to NAIP (Speijer and Wagner, 2002; Sluijs et al., 2008; Bowen and Zachos, 2010;
495 Khozyem et al., 2015).

496 At the PEB planktic foraminifera suddenly disappeared and calcite decreased to
497 near 0 % for 42 cm in the lower part of zone E1 followed by a brief reappearance of
498 calcite (35 %) and small opportunistic new foraminiferal species and radiolarians (Figs.
499 13A, 14). Above this interval calcite varies between 10-30 % but planktic foraminifera
500 are generally rare to absent and reappearing only with calcite content >40 % at the top of
501 zone E1 (Fig. 14).

502 The sudden calcite drop at the PEB from 50 % to near 0 % coincides with onset of
503 high detrital input during the PETM interval that spans zone E1 (Figs. 13, 14). Khozyem
504 et al. (2015, p. 127) argued that *"detrital input negatively affects the calcite content*

resulting in minimum values that could be due to leaching of carbonate contents under acid conditions and/or dilution by increased detrital input." The high terrigenous input at Dababiya due to climate and sea level changes supports this interpretation (e.g., Khozyem et al., 2015; Schulte et al., 2011; Speijer and Wagner, 2002). The temporary absence of benthic and planktic foraminifera and near absence of nannofossils during the PETM coupled with shoaling of the CCD by 2000 m indicates ocean acidification likely due to a huge rapid input of CO_2 from methane degassing (e.g., Zachos et al., 2008; Westerhold et al., 2011) and/or from NAIP volcanism (Gutjahr et al., 2017).

6. DISCUSSION

6.1. PETM Event

During the Paleocene-Eocene transition two major volcanic events temporally precede and overlap the PETM (~55.8 ± 0.2 Ma; Westerhold et al., 2009; Charles et al., 2011; Wieczorek et al., 2013) (Fig. 1B): (1) the North Atlantic Igneous Province (NAIP) formed during the opening of the northern part of the North Atlantic ocean ~61 Ma with maximum activity between 57 and 54 Ma (Hirschman et al, 1997; Svensen et al., 2004, 2010; Storey et al., 2007); and (2) Central American circum-Caribbean volcanism linked to enhanced tectonic activity that began ~56-55.5 Ma in the proto Greater Antilles (Sigurdsson et al., 1997). Thus the nature of NAIP volcanism associated with the PETM event was fundamentally different from the continental flood basalt Deccan Traps eruptions.

Support for NAIP as driver for the PETM comes from a large drop in $^{187}Os/^{188}Os$ and ash deposits dated ~24 ky before the maximum $\delta^{13}C$ excursion in Core BH9/05 (Spitsbergen, Svalbard Archipelago, Norway) (Wieczorek et al., 2013) and from an Earth system model pairing ocean surface pH data and a carbon isotope record from the northeast Atlantic Ocean (Gutjahr et al., 2017). Recent discovery of Hg anomalies in North Atlantic, Spain and Egypt provide further evidence linking NAIP to the PETM event by initiating the warming that likely led to the release of methane gases from organic-rich sediments (Svensen et al., 2004, 2010; Maclennan and Jones, 2006; Wieczorek et al., 2013).

The PETM event was a short-term and isolated event possibly triggered by an estimated ~2000 Gt of CO_2 from volcanic activity (NAIP, Sinton and Duncan, 1998; Westerhold et al., 2011) and ~1500 Gt of methane carbon from gas hydrates released into the atmosphere (Dickens et al., 1995; Dickens, 2003). (These CO_2 estimates are based on the $\delta^{13}C$ isotope excursion, which may have large uncertainties.) The resulting rapid global warming is thought to have occurred over about ~10 ky with the entire event lasting ~170 ky. This suggests rapid injection of carbon and slow subsequent removal given that the average residence time of carbon in the ocean is about 100 ky (Zachos et al., 2005, 2008). Boron-based ($\delta^{11}B$ and B/Ca) proxies for surface ocean carbonate chemistry indicate an estimated ~0.3 units drop in the pH of surface and thermocline seawater sustained over ~70 ky during the PETM (Penman et al., 2014). Model simulations suggest that this duration is consistent with a scenario of rapid initial pulse of carbon loading followed by continued slow, gradual release of carbon likely due to feedbacks (Panchuk et al., 2008; Zeebe et al., 2009; Zeebe, 2012).

The PETM coincides with ocean acidification and shoaling of the CCD by 2000 m (Zachos et al., 2005, 2008; Speijer and Wagner, 2002; Sluijs et al., 2008; Gutjahr et al., 2017); the latter may account for benthic foraminifera extinctions in deep waters (Thomas, 1998; Alegret et al., 2006). Planktic foraminifera and calcareous nannofossils temporarily disappeared from tropical and subtropical oceans (suggesting warming and surface ocean acidification) by migrating into higher latitudes. Assemblages returned after the PETM with no significant extinctions and underwent evolutionary diversification (Lu and Keller, 1993, 1995a, b; Kelly et al., 1996, 1998; Luciani et al., 2007, 2016; Khozyem et al., 2014). On land extreme climate warming resulted in decreased abundances and dwarfing ranging from soil dwelling species (e.g., burrowers, crayfish, mollusks, Smith et al., 2009) to mammals (D'Ambrosia et al., 2017). But the great mammal migration, diversification and geographic dispersal began shortly after the PETM (Koch et al., 1992, 1995; Hooker, 1998; Clyde and Gingrich, 1998; Clyde et al., 2003; Tong and Wang, 2006; Smith et al., 2006; Rose et al., 2008; Punekar and Saraswati, 2010; Smith, 2012).

6.2. KPB Event

The main phase of Deccan volcanism spans magnetochron C29r (Chenet et al., 2008, 2009) dated ~750 ky during which time an estimated >1.1 million km^3 of basalt erupted (Schoene et al., 2015). The KPB is at 66.021±0.024 Ma, ~350 ky after the onset of eruptions at the base of C29r. Hg anomalies and Hg/TOC ratios at Elles indicate that volcanic eruptions accelerated during the last 40 ky before the mass extinction (Fig. 10). In the field in India, Deccan eruptions near the end of the Maastrichtian resulted in 3-4

lava megaflows that flowed over 1000 km across India into the Bay of Bengal (Keller et al., 2011a; Self et al., 2008) (Fig. 1A). The mass extinction of planktic foraminifera was documented directly in sediments between these lava megaflows in cores 2500-3500 m below the surface in the Krishna-Godavari Basin (Keller et al., 2011a, 2012). Danian (zone P1a) sediments overlie the megaflows and constrain the age of the KPB mass extinction to peak volcanic activity, as now confirmed by the large Hg/TOC ratios at Elles (Fig. 10). An estimated cumulative loading of 12,000-28,000 Gt of volcanogenic CO_2 spewed into the end-Cretaceous atmosphere within less than 350 ky and significantly increased atmospheric pCO_2 (Courtillot and Fluteau, 2014; Self et al., 2014). Volcanic eruptions continued intermittently through the early Danian C29r with the last phase of eruptions in the lower part of C29n (Fig. 11). Mercury analysis in marine and terrestrial sediments worldwide mark late Maastrichtian and early Danian Deccan eruptions linked directly to the KPB mass extinction (Font et al., 2016; this study).

Rapid climate warming of 3-4 ºC during massive Deccan eruptions resulted in dwarfed planktic foraminifera and reduced abundances of all but a few stress-resistant taxa dominated by a single disaster opportunist and sole long-term survivor *Guembelitria cretacea* (Keller and Abramovich, 2009). On land, non-avian dinosaurs, mammals, amphibians, plants and insects (e.g., MacLeod et al., 1997; Labandeira et al., 2002; Wilf and Johnson, 2004; Wilson et al., 2005, 2014; Nichols and Johnson, 2008; Longrich et al., 2011, 2012; Wilson, 2014; Vajda and Bercovici, 2014; Donovan et al., 2016) also recorded a prolonged ecological decline, reduced diversity and turnovers during climate instability associated with Deccan volcanism preceding the KPB (e.g., Wilf and Johnson, 2004; Wilson, 2005, 2014; Wilson et al., 2014; Archibald, 1996, 2011).

596 The similar patterns of long-term stress and decline in marine and terrestrial
597 faunas and flora during the late Maastrichtian C29r warming parallels massive Deccan
598 volcanism that accelerated during the last 10 ky leading to further warming and probably
599 reaching threshold conditions. Maximum volcanic eruptions in rapid succession during
600 the last few thousand years culminated with the KPB mass extinction (Fig. 10). The
601 subsequent delayed recovery in marine plankton and on land can now be shown to
602 coincide with continued though less frequent Deccan volcanic eruptions keeping stress
603 conditions high (Fig. 11). Deccan volcanism is thus a major culprit for climate warming,
604 biotic stresses and the mass extinction.

605 The Chicxulub impact is commonly believed to be the sole cause for the KPB
606 mass extinction based primarily on the Ir anomaly in the KPB clay layer, the imPACT
607 CRATER IN MEXICO AND IMPACT GLASS SPHERULES FREQUENTLY FOUND IN
608 SEDIMENTS AT, BELOW OR ABOVE THE KPB, WHICH HAS BEEN THE SOURCE OF
609 CONTROVERSY (SCHULTE ET AL., 2010; KELLER ET AL., 2011B). (SEE
610 SUPPLEMENTARY MATERIALS S3 FOR A DISCUSSION OF THIS CONTROVERSY.)
611 HOWEVER, OVER THE PAST 10 YEARS, INCREASING EVIDENCE LINKING THE MASS
612 EXTINCTION TO DECCAN VOLCANISM REVEALS THE NEED FOR RE-EVALUATION
613 OF THE IMPACT THEORY. CRITICAL EVIDENCE LINKING THE MASS EXTINCTION
614 DIRECTLY TO DECCAN VOLCANISM INCLUDES: (1) THE MASS EXTINCTION
615 DOCUMENTED BETWEEN MASSIVE LAVA FLOWS IN INDIA DIRECTLY BELOW THE
616 KPB (KELLER ET AL., 2008, 2009, 2011A, 2012), (2) U-PB AGE DATING OF ASH
617 LAYERS AND RED BOLE INTERTRAPPEAN SEDIMENTS THAT SPAN C29R (SCHOENE
618 ET AL., 2015), AND (3) HG ANOMALIES THAT MARK ATMOSPHERIC FALLOUT
619 FROM DECCAN ERUPTIONS WORLDWIDE (SILVA ET AL., 2013; FONT ET AL., 2016;

620 THIS STUDY). AS A RESULT, THE IMPACT THEORY IS ALREADY BEING MODIFIED
621 BY IMPACT PROPONENTS SUGGESTING THAT THE IMPACT TRIGGERED DECCAN
622 VOLCANISM (RICHARDS ET AL., 2015), OR ACCELERATED DECCAN VOLCANISM
623 LEADING TO EXTINCTIONS (RENNE ET AL., 2015). THE PRECISE AGE OF THE
624 CHICXULUB IMPACT IS CURRENTLY UNDER INVESTIGATION BASED ON NEW
625 AR/AR DATING OF IMPACT SPHERULES BY THREE LABORATORIES. THE PRECISE
626 ROLE THE IMPACT PLAYED IN THE MASS EXTINCTION ALSO STILL REMAINS TO BE
627 DETERMINED IN LIGHT OF NEW DECCAN VOLCANISM DATA. WHAT IS CERTAIN IS
628 THAT THIS IMPACT ADDED A SIGNIFICANT BLOW TO AN ALREADY WEAKENED
629 AND STRESSED ENVIRONMENT REGARDLESS OF THE PRECISE AGE. BUT IT WAS A
630 ONE-TIME BLOW AT THE LEVEL OF TOTAL CO_2 AND SO_2 GAS OUTPUT
631 COMPARABLE TO ONE MAJOR DECCAN ERUPTION PULSE OF WHICH THERE ARE
632 MANY (CHENET ET AL., 2008; COURTILLOT AND FLUTEAU, 2014).

633 At present we can confidently evaluate the PETM and KPB catastrophes based on
634 the response by planktic foraminifera, which are an essential part of the food chain, and
635 new Hg anomaly data now link these global faunal records to NAIP and Deccan
636 volcanism. The fundamentally different biotic responses to these catastrophes lie in the
637 nature of volcanic eruptions. During the PETM, NAIP volcanism due to rifting of the
638 North Atlantic led to relatively short-term gradual warming that likely triggered the
639 postulated methane release and rapid warming. Absence of Hg anomalies after the PETM
640 indicates no significant NAIP eruptions, climate cooled and biotic recovery was rapid. In
641 contrast, Deccan Traps are continental flood basalt eruptions that began ~350 ky before
642 the KPB mass extinction causing long-term warming. Accelerating eruptions during the

643 last ~10 ky reached the tipping point and mass extinction. Thereafter, intermittent Deccan
644 eruptions delayed recovery for over 500 ky.
645
646 **6.3. Anthropocene: The Sixth Mass Extinction?**
647 Scientists increasingly recognize the accelerating rate of modern species
648 extinctions and sounding alarm that humans are now causing the sixth mass extinction
649 (e.g., Leakey and Lewin, 1992; Dirzo and Raven, 2003; Wake and Vredenburg, 2008;
650 Barnosky et al., 2011; Glikson, 2014). Evidence of an impending catastrophe is all
651 around us in the increasing rate of species extinctions and those endangered on the verge
652 of extinction. Climate warming due to fossil fuel burning is attributed to the increasing
653 rate of extreme climate events, melting of polar glaciers and rapidly rising sea level.
654 Despite all this, it is hard to fathom that we are living in the midst of a mass extinction.
655 We can glimpse our future from comparison with extreme events in the past,
656 particularly the hyperthermal warming (PETM) of the Paleocene-Eocene boundary (PEB,
657 55.8 Ma) and rapid extreme warming leading to the end-Cretaceous mass extinction
658 (KPB, 66.0 Ma) (Table 1). Both PEB and KPB catastrophes are largely the results of
659 massive rapid emissions of greenhouse gases leading to the tipping point. At one
660 extreme, scientists suggest the tipping point may have already been reached at the current
661 CO_2 level (407 ppm) and that just 1 °C additional warming may result in runaway
662 warming, ocean acidification and the sixth mass extinction (Glikson, 2014). At the other
663 extreme are those who deny the existence of current climate change.
664 Projecting current and/or increasing Anthropocene warming into the future has
665 the potential to follow the path of the PETM hyper-warming and faunal turnover, as

666 frequently suggested by scientists, or it could end in a mass extinction similar to the KPB
667 as suggested by predictions of the sixth mass extinction. Global climate warming due to
668 massive input of greenhouse gases is the leading cause for all three events even if the
669 sources differ (Table 1). Critical is the rapid rate of climate warming that is vastly (12 to
670 16 times) more rapid for the Anthropocene. The tipping point may be around 5 °C and
671 just 1 °C off from the current overall temperature rise (Hay, 2011).

672 Ocean acidification and acid rain on land had catastrophic effects for PETM and
673 KPB events and similar effects are already ongoing today. For example, seasonal
674 aragonite undersaturation observed in surface waters of the Southern Ocean already have
675 harmful effects on live pteropods (Bednarsek et al., 2012; Hunt et al., 2008; Sunday et al.,
676 2014). By 2030 undersaturation is predicted to spread to ~30 % of the Southern Ocean
677 and >70 % by 2100 as a result of anthropogenic CO_2, thus severely affecting the marine
678 food chain (McNeil and Matear, 2008; Hauri et al., 2016).

679 A cartoon illustrates the nature of the three events (Fig. 15). Climate warming and
680 the end-Cretaceous mass extinction are closely linked to the Chicxulub impact and
681 Deccan volcanism (Fig. 15A). The latter emitted huge quantities of aerosols and
682 greenhouse gases (CO_2, SO_2) into the atmosphere over 350 ky and the impact added in a
683 single instant a quantity about equal to one major Deccan eruption pulse (Chenet et al.,
684 2008; Courtillot and Fluteau, 2014). Accelerating large volcanic eruptions during the last
685 10 ky prior to the mass extinction led to increased warming and the tipping point
686 resulting in the rapid mass extinction of 66 % planktic foraminiferal species during the
687 last few thousand years of the Cretaceous, followed by another 33 % within 50-150 ky in

688 the early Danian. Continued eruptions in the early Danian delayed full recovery for over
689 500 ky.

690 The PEB event can be attributed to NAIP volcanism and climate warming that
691 likely set the conditions for the abrupt release of methane (CH_4) stored in organic-rich
692 sediments on land and continental shelves resulting in the rapid PETM warming of 5 °C
693 within ~10 ky (Fig. 15B). Methane, partially oxidized in the water column leading to
694 ocean acidification during the relatively short but intense PETM event (~170 ky) raising
695 the CCD by 2000 m. Prevailing hot-humid conditions on land and recovery of carbonate
696 deposition via CO_2 drawdown by organic matter burial in the oceans are likely causes for
697 the rapid return/recovery and diversification of marine faunas after the PETM (Bains et
698 al., 2000).

699 Current rapid warming is the result of huge inputs of greenhouse gases (CO_2,
700 CH_4) linked to human activities and fossil fuel burning during the Anthropocene (Fig.
701 15C). The input rate of greenhouse gases exceeds those at the PETM and KPB by orders
702 of magnitude. Ozone depletion and particle pollution from fossil fuel burning and other
703 human activities result in dust clouds that trap solar radiation in Earth's atmosphere with
704 little reflected back into space, thus contributing to Earth's rising temperature. Similar to
705 PEB and KPB events, today's CO_2 from the atmosphere is absorbed in the oceans and has
706 already lowered the pH; ocean acidification is already affecting shelly organisms at the
707 base of the food chain (e.g., pteropods, corals) and endangering all life up the food chain.
708 At the current trend of greenhouse gas emissions, the prediction is that Cretaceous-like
709 climate could be reached by 2070 setting us well on the way to the sixth mass extinction
710 within as little as a couple of hundred years (Hay, 2011; Hauri et al., 2016).

The worst-case scenario could thus be similar to the KPB mass extinction but with a faster rate of extinctions; this is currently predicted as the Anthropocene mass extinction – or sixth mass extinction. The best-case scenario could be similar to the PETM event: We escape mass extinctions but suffer through a period of extreme environmental stress marked by intense heat, extreme climate events, rising sea level and severe food shortages reducing populations and forcing migration to higher latitudes for survival. This scenario depends on dramatically reducing greenhouse gas input thus slowing the rate of global warming and its dire long-term consequences.

7. CONCLUSIONS

The PETM extreme warming is a commonly used analogue and predicted best-case scenario for the current rapid climate warming in the coming decades and centuries. If this is our fate, survival is possible although in reduced populations with the best chances for survival in higher latitudes. The predicted worst-case scenario for the current climate trend is the sixth mass extinction. The KPB mass extinction is a good analogue for this catastrophic scenario because accelerating Deccan volcanic eruptions and increasing greenhouse gas input into the atmosphere can have similar effects on the biosphere as current fossil-fuel burning. Perhaps all it takes to realize the sixth mass extinction scenario is continued or increasing greenhouse gas input reaching the tipping point. It is unclear whether current climate warming will follow the PETM or KPB analogue, or a completely different model of biosphere destruction unseen in Phanerozoic mass extinctions.

ACKNOWLEDGMENTS

We thank G.R. Dickens, S. Ashckenazi-Polivoda and four anonymous reviewers for their comments and critiques, which have greatly helped improve this paper. This study is based upon work supported by Princeton University, Geosciences Department Tuttle and Scott funds, the US National Science Foundation through the Continental Dynamics Program (Leonard Johnson), Sedimentary Geology and Paleobiology Program and Office of International Science & Engineering's India Program under NSF grants EAR-0207407, EAR-0447171, EAR-1026271 and INT 95-04309.

REFERENCES

Abramovich, S., and Keller, G., 2002. High stress late Maastrichtian paleoenvironment: inference from planktonic foraminifera in Tunisia. Palaeogeography, Palaeoclimatology, Palaeoecology, 178, 145-164, doi:10.1016/S0031-0182(01)00394-7.

Abramovich, S., and Keller, G., 2003. Planktonic foraminiferal response to the latest Maastrichtian abrupt warm event: A case study from South Atlantic DSDP Site 525A. Marine Micropaleontology, 48, 225-249, doi:10.1016/S0377-8398(03)00021-5.

Abramovich, S., Keller, G., Stu□ben, D., and Berner, Z., 2003. Characterization of late Campanian and Maastrichtian planktonic foraminiferal depth habitats and vital activities based on stable isotopes. Palaeogeography, Palaeoclimatology, Palaeoecology, 202, 1-29, doi:10.1016/S0031-0182(03)00572-8.

Abramovich, S., Yovel-Corem, S., Almogi-Labin, A., and Benjamini, C., 2010. Global climate change and planktic foraminiferal response in the Maastrichtian. Paleoceanography, 25, PA2201, doi:10.1029/2009PA001843.

Adatte, T., Keller, G., and Stinnesbeck, W., 2002. Late Cretaceous to early Paleocene climate and sea-level fluctuations: the Tunisian record. Palaeogeography, Palaeoclimatology, Palaeoecology, 178(3), 165-196, doi:10.1016/S0031-0182(01)00395-9.

772 Alegret, L., and Ortiz, S., 2006. Global extinction event in benthic foraminifera across the
773 Paleocene/Eocene boundary at the Dababiya Stratotype section. Micropaleontology,
774 52(5), 48-63, doi:10.2113/gsmicropal.52.5.433.
775 Alegret, L., Ortiz, S., Arenillas, I., Molina, E., 2005. Paleoenvironmental turnover across
776 the Paleocene/Eocene Boundary at the Stratotype section in Dababiya (Egypt)
777 based on benthic foraminifera. Terra Nova, 17, 526-536.
778 Alegret, L., Ortiz, S., Molina, E., 2009. Extinction and recovery of benthic foraminifera
779 across the Paleocene–Eocene ThermalMaximum at the Alamedilla section
780 (Southern Spain). Palaeogeography, Palaeoclimatology, Palaeoecology, 279, 186-
781 200, doi:10.1016/j.palaeo.2009.05.009.
782 Archibald, J.D., 1996. Testing extinction theories at the Cretaceous-Tertiary boundary
783 using the vertebrate fossil record. In: MacLeod, N., Keller, G. (Eds.), Cretaceous-
784 Tertiary Mass Extinctions: Biotic and Environmental Changes. WW Norton &
785 Company, New York/London, pp. 373-397.
786 Archibald, J.D., 2011. Extinction and radiation: how the fall of dinosaurs led to the rise of
787 mammals. JHU Press, p. 108.
788 Ashckenazi-Polivoda, S., Abramovich, S., Almogi-Labin, A., Schneider-Mor, A.,
789 Feinstein, S., Pu□ttmann, W., and Berner, Z., 2011. Paleoenvironments of the latest
790 Cretaceous oil shale sequence, Southern Tethys, Israel, as an integral part of the
791 prevailing upwelling system. Palaeogeography, Palaeoclimatology, Palaeoecology,
792 305(1), 93-108, doi:10.1016/j.palaeo.2011.02.018.
793 Aubry, M.-P., Ouda, K., Dupuis, C., Berggren, W.A., Van Couvering, J.A., and the
794 Members of the Working Group on the Paleocene/Eocene Boundary, 2007. Global

795 Standard Stratotype – Section and Point (GSSP) for the base of the Eocene Series in
796 the Dababiya Section (Egypt). Episodes, 30(4), 271-286.
797 Bains, S., Norris, R.D., Corfield, R.M., Faul, K.L., 2000, Termination of global warmth
798 at the Palaeocene/Eocene boundary through productivity feedback. Nature, 407,
799 171-174, doi:10.1038/35025035.
800 Barnosky, A.D., Matzke, N., Tomiya, S., Wogan, G.O., Swartz, B., Quental, T.B.,
801 Marshall, C., McGuire, J.L., Lindsey, E.L., Maguire, K.C., and Mersey, B., 2011.
802 Has the Earth's sixth mass extinction already arrived? Nature, 471(7336), 51-57.
803 Barrera, E., and Keller, G., 1990. Stable isotope evidence for gradual environmental
804 changes and species survivorship across the Cretaceous/Tertiary boundary.
805 Paleoceanography, 5, 867-890, doi:10.1029/PA005i006p00867.
806 Bednarsek, N., Tarling, G.A., Bakker, D.C.E., Fielding, S., Jones, E.M., Venables, H.J.,
807 Ward, P., Kuzirian, A., Lézé, B., Feely, R.A., and Murphy, E.J., 2012. Extensive
808 dissolution of live pteropods in the Southern Ocean. Nature Geoscience, 5(12), 881-
809 885, doi:10.1038/ngeo1635.
810 Begon, M., Mortimer, M., and Thompson, D.J., 1996. Population Ecology: A Unified
811 Study of Plants and Animals. Cambridge, UK, Blackwell, 247 p.
812 Begon, M., Harper, J.L., and Townsend, C.R., 1998. Ecology: Individuals, Populations
813 and Communities. Boston, Blackwell Science, 1068 p.
814 Berggren, W.A., and Ouda, K., 2003. Upper Paleocene–lower Eocene planktonic
815 foraminiferal biostratigraphy of the Dababiya section, Upper Nile Valley (Egypt).
816 In: Ouda, K., Aubry, M.-P. (Eds.), The Upper Paleocene–Lower Eocene of the

817 Upper Nile Valley: Part 1, Stratigraphy. Micropaleontology, 49, 61-92 (supplement
818 1), doi:10.2113/49.Suppl_1.61.
819 Borths, M.R., and Ausich, W.I., 2011. Ordovician–Silurian Lilliput crinoids during the
820 end-Ordovician biotic crisis. Swiss Journal of Palaeontology, 130(1), 7-18,
821 doi:10.1007/s13358-010-0003-2.
822 Bosetti, E.P., Grahn, Y., Horodyski, R.S., Mauller, P.M., Breuer, P., and Zabini, C.,
823 2010. An earliest Givetian "Lilliput Effect" in the Paraná Basin, and the collapse of
824 the Malvinokaffric shelly fauna. Paläontologische zeitschrift, 85(1), 49-65, doi:
825 10.1007/s12542-010-0075-8.
826 Bowen, G.J., and Zachos, J.C., 2010. Rapid carbon sequestration at the termination of the
827 Palaeocene-Eocene Thermal Maximum. Nature Geoscience, 3, 866-869,
828 doi:10.1038/ngeo1014.
829 Ceballos, G., and Ehrlich, P.R., 2002. Mammal population losses and the extinction
830 crisis. Science, 296, 904-907, doi:10.1126/science.1069349.
831 Charles, A.J., Condon, D.J., Harding, I.C., Pälike, H., Marshall, J.E., Cui, Y., Kump, L.,
832 and Croudace, I.W., 2011. Constraints on the numerical age of the Paleocene-
833 Eocene boundary. Geochemistry, Geophysics, Geosystems, 12(6),
834 doi:10.1029/2010GC003426.
835 Chenet, A.-L., Fluteau, F., Courtillot, V., Gérard, M., and Subbarao, K.V., 2008.
836 Determination of rapid Deccan eruptions across the Cretaceous-Tertiary boundary
837 using paleomagnetic secular variation: results from a 1200-m-thick section in the
838 Mahabaleshwar escarpment. Journal of Geophysical Research: Solid Earth,
839 113(B4), doi:10.1029/2006JB004635.

840 Chenet, A.-L., Courtillot, V., Fluteau, F., Gerard, M., Quidelleur, X., Khadri, S.F.R.,
841 Subbarao, K.V., Thordarson, T., 2009. Determination of rapid Deccan eruptions
842 across the Cretaceous-Tertiary boundary using paleomagnetic secular variation: 2.
843 Constraints from analysis of eight new sections and synthesis for a 3500-m-thick
844 composite section. Journal of Geophysical Research, 114, B06103,
845 doi:10.1029/2008JB005644.
846 Chu, D., Tong, J., Song, H., Benton, M.J., Song, H., Yu, J., Qiu, X., Huang, Y., Tian, L.,
847 2015. Lilliput effect in freshwater ostracods during the Permian–Triassic extinction.
848 Palaeogeography, Palaeoclimatology, Palaeoecology, 435, 38-52,
849 doi:10.1016/j.palaeo.2015.06.003.
850 Clyde, W.C., and Gingerich, P.D., 1998. Mammalian community response to the latest
851 Paleocene thermal maximum: An isotaphonomic study in the northern Bighorn
852 Basin, Wyoming. Geology, 26, 1011-1014, doi:10.1130/0091-7613(1998)
853 026<1011:MCRTTL>2.3.CO;2.
854 Clyde, W.C., Khan, I.H., and Gingerich, P.D., 2003. Stratigraphic response and
855 mammalian dispersal during initial India-Asia collision: Evidence from the Ghazij
856 Formation, Balochistan, Pakistan. Geology, 31(12), 1097-1100,
857 doi:10.1130/G19956.1.
858 Coccioni, R., and Luciani, V., 2006. *Guembelitria irregularis* bloom at the K-T
859 boundary: Morphological abnormalities induced by impact-related extreme
860 environmental stress? In: Cockell, C., Koeberl, C., Gilmour, I. (Eds.), Biological
861 Processes Associated with Impact Events. Impact Studies, Berlin, Springer, 179-
862 196.

Coccioni, R., Bancala, G., Catanzarit, R., Fornaciari, E., Frontalini, F., Giusberti, L., Jovane, L., Luciani, V., Savian, J., andSprovieri, M., 2012. An integrated stratigraphic record of the Palaeocene–lower Eocene at Gubbio (Italy): new insights into the early Palaeogene hyperthermals and carbon isotope excursions. Terra Nova, 24(5), 380-386, doi:10.1111/j.1365-3121.2012.01076.x.

Courtillot, V., and Fluteau, F., 2014. A review of the embedded time scales of flood basalt volcanism with special emphasis on dramatically short magmatic pulses. In: Keller, G., and Kerr, A.C. (Eds.), Volcanism, Impacts, and Mass Extinctions: Causes and Effects. Geological Society of America Special Paper, 505, 301-317, doi:10.1130/2014.2505(15).

Cowie, J.W., Ziegler, W., and Remane, J., 1989. Stratigraphic Commission accelerates progress, 1984 to 1989. Episodes, 12, 79-83.

Culver, S.J., 2003. Benthic foraminifera across the Cretaceous–Tertiary (K–T) boundary: a review. Marine Micropaleontology, 47(3), 177-226, doi:10.1016/S0377-8398(02)00117-2.

D'Ambrosia A.R., Clyde, W.C., Fricke, H.C., Gingerich, P.D., and Abels, H.A., 2017. Repetitive mammalian dwarfing during ancient greenhouse warming events. Science Advances, 3(3), e1601430, doi:10.1126/sciadv.1601430.

da Silva, A.C., Potma, K., Weissenberger, J.A., Whalen, M.T., Humblet, M., Mabille, C., and Boulvain, F., 2009. Magnetic susceptibility evolution and sedimentary environments on carbonate platform sediments and atolls, comparison of the Frasnian from Belgium and Alberta, Canada. Sedimentary Geology, 214(1), 3-18, doi:10.1016/j.sedgeo.2008.01.010.

886 Dickens, G.R., 2000. Methane oxidation during the late Palaeocene thermal maximum.
887 Bulletin de la Société géologique de France, 171(1), 37-49.
888 Dickens, G.R., 2003. Rethinking the global carbon cycle with a large, dynamic and
889 microbially mediated gas hydrate capacitor. Earth and Planetary Science Letters,
890 213, 169-183, doi:10.1016/S0012-821X(03)00325-X.
891 Dickens, G.R., O'Neil, J.R., Rea, D.C., and Owen, R.M., 1995. Dissociation of oceanic
892 methane hydrate as a cause of the carbon isotope excursion at the end of the
893 Paleocene. Paleoceanography, 10, 965-971, doi:10.1029/95PA02087.
894 Dirzo, R., and Raven, P.H., 2003. Global state of biodiversity and loss. Annual Review of
895 Environment and Resources, 28(1), 137-167.
896 Donovan, M.P., Iglesias, A., Wilf, P., Labandeira, C.C., and Cúneo, N.R., 2016. Rapid
897 recovery of Patagonian plant–insect associations after the end-Cretaceous
898 extinction. Nature Ecology & Evolution, 1, 0012, doi:10.1038/s41559-016-0012.
899 Dupuis, C., Aubry, M.-P., Steurbaut, E., Berggren, W.A., Ouda, K., Magioncalda, R.,
900 Cramer, B.S., Kent, D.V., Speijer, R.P., and Heilmann-Clausen, C., 2003. The
901 Dababiya Quarry section: lithostratigraphy, clay mineralogy, geochemistry and
902 paleontology. In: Ouda, K., Aubry, M.-P. (Eds.), The Upper Paleocene–Lower
903 Eocene of the Upper Nile Valley: Part 1.Stratigraphy. Micropaleontology, 49, 41-
904 59, doi:10.2113/49.Suppl_1.41.
905 Feduccia, A., 2014. Avian extinction at the end of the Cretaceous: Assessing the
906 magnitude and subsequent explosive radiation. Cretaceous Research, 50, 1-15,
907 doi:10.1016/j.cretres.2014.03.009.

908 Font, E., Nédélec, A., Ellwood, B.B., Mirão, J., and Silva, P.F., 2011. A new sedimentary
909 benchmark for the Deccan Traps volcanism? Geophysical Research Letters, 38(24),
910 L24309, doi:10.1029/2011GL049824.
911 Font, E., Fabre, S., Nédélec, A., Adatte, T., Keller, G., Veiga-Pires, C., Ponte, J., Mirão,
912 J., Khozyem, H., and Spangenberg, J.E., 2014. Atmospheric halogen and acid rains
913 during the main phase of Deccan eruptions: magnetic and mineral evidence.
914 Geological Society of America Special Paper, 505, 353-368,
915 doi:10.1130/2014.2505(18).
916 Font, E., Adatte, T., Sial, A.N., de Lacerda, L.D., Keller, G., and Punekar, J., 2016.
917 Mercury anomaly, Deccan volcanism, and the end-Cretaceous mass extinction.
918 Geology, 44(2), 171-174, doi: 10.1130/G37451.1.
919 Glikson, A.Y., 2014. Evolution of the Atmosphere, Fire and the Anthropocene Climate
920 Event Horizon. Springer Netherlands, pp. 174, doi:10.1007/978-94-007-7332-5.
921 Gong, Q., Wang, X., Zhao, L., Grasby, S.E., Chen, Z.Q., Zhang, L., Li, Y., Cao, L., and
922 Li, Z., 2017. Mercury spikes suggest volcanic driver of the Ordovician-Silurian
923 mass extinction. Scientific Reports, 7, 5304, doi:10.1038/s41598-017-05524-5.
924 Gradstein, F.M., Ogg, J., and Smith, A., 2004. A Geologic Time Scale. Cambridge, U.K.,
925 Cambridge University Press, pp. 598, ISBN-13: 9780511074059.
926 Grasby, S.E., Sanei, H., Beauchamp, B., and Chen, Z.H., 2013. Mercury deposition
927 through the Permo-Triassic biotic crisis. Chemical Geology, 351, 209-216,
928 doi:10.1016/j.chemgeo.2013.05.022.
929 Gutjahr, M., Ridgwell, A., Sexton, P.F., Anagnostou, E., Pearson, P.N., Pälike, H.,
930 Norris, R.D., Thomas, E., and Foster, G.L., 2017. Very large release of mostly

volcanic carbon during the Palaeocene-Eocene Thermal Maximum. Nature, 548(7669), 573-577, doi:10.1038/nature23646.

Hauri, C., Friedrich, T., and Timmermann, A., 2016. Abrupt onset and prolongation of aragonite undersaturation events in the Southern Ocean. Nature Climate Change, 6(2), 172-176, doi:10.1038/nclimate2844.

Hay, W.W., 2011. Can humans force a return to a 'Cretaceous' climate? Sedimentary Geology, 235, 5-26, doi:10.1016/j.sedgeo.2010.04.015.

Hirschmann, M.M., Renne, P.R., and McBirney, A.R., 1997. 40Ar/39Ar dating of the Skaergaard intrusion. Earth and Planetary Science Letters, 146, 645-658. doi: 10.1016/S0012-821X(96)00250-6.

Hönisch, B., Ridgwell, A., Schmidt, D.N., Thomas, E., Gibbs, S.J., Sluijs, A., Zeebe, R., Kump, L., Martindale, R.C., Greene, S.E., Kiessling, G., Ries, J., Zachos, J.C., Royer, D.L., Barker, S., Marchitto, T.M., Jr., Moyer, R., Pelejero, C., Ziveri1, P., Foster, G.L., and Williams, B., 2012. The geological record of ocean acidification. Science, 335(6072), 1058-1063, doi:10.1126/science.1208277.

Hooker, J.J., 1998. Mammalian faunal change across the Paleocene-Eocene transition in Europe. In: Aubry, M.P., Lucas, S., Berggren, W.A. (Eds.), Late Paleocene-Early Eocene Climatic and Biotic Events in the Marine and Terrestrial Records. New York, Columbia University Press, pp. 428-450.

Hughes, J.B., Daily, G.C., and Ehrlich, P.R., 1997. Population diversity: its extent and extinction. Science, 278, 689-692, doi:10.1126/science.278.5338.689.

953 Hunt, B.P.V., Pakhomov, E.A., Hosie, G.W., Siegel, V., Ward, P., and Bernard, K., 2008.
954 Pteropods in southern ocean ecosystems. Progress in Oceanography, 78(3), 193-
955 221, doi:10.1016/j.pocean.2008.06.001.
956 IPCC, 2007. Climate Change 2007: The Physical Science Basis. Contribution of Working
957 Group I to the Fourth Assessment Report of the Intergovernmental Panel on
958 Climate Change. Solomon, S., Qin, D., Manning, M., Chen, Z., Marquis, M.,
959 Averyt, K.B., Tignor, M., Miller, H.L. (Eds.) Cambridge University Press,
960 Cambridge, United Kingdom and New York, NY, USA.
961 IPCC, 2013. Climate Change 2013: The Physical Science Basis. Contribution of Working
962 Group I to the Fifth Assessment Report of the Intergovernmental Panel on Climate
963 Change. Stocker, T.F., Qin, D., Plattner, G.-K., Tignor, M., Allen, S.K., Boschung,
964 J., Nauels, A., Xia, Y., Bex, V., Midgley, P.M. (Eds.). Cambridge University Press,
965 Cambridge, United Kingdom and New York, NY, USA.
966 Kaiho, K., Takeda, K., Petrizzo, M.R., and Zachos, J.C., 2006. Anomalous shifts in
967 tropical Pacific planktonic and benthic foraminiferal test size during the Paleocene–
968 Eocene thermal maximum. Palaeogeography, Palaeoclimatology, Palaeoecology,
969 237(2), 456-464, doi: 10.1016/j.palaeo.2005.12.017.
970 Keller, G., 1988a. Extinction, survivorship and evolution of planktic foraminifers across
971 the Cretaceous/Tertiary boundary at El Kef, Tunisia. Marine Micropaleontology,
972 13, 239-263, doi:10.1016/0377-8398(88)90005-9.
973 Keller, G., 1988b. Biotic turnover in benthic foraminifera across the Cretaceous/Tertiary
974 boundary at El Kef, Tunisia. Palaeogeography, Palaeoclimatology, Palaeoecology,
975 66(3-4), 153-171, doi:10.1016/0031-0182(88)90198-8.

976 Keller, G., 1992. Paleoecologic response of Tethyan benthic Foraminifera to the
977 Cretaceous-Tertiary boundary transition. In: Takayanagi, Y., Saito, T. (Eds.), Studies in
978 Benthic Foraminifera. Tokai University Press, Tokyo, p. 77-91.
979 Keller, G., 2001. The end-cretaceous mass extinction in the marine realm: year 2000
980 assessment. Planetary and Space Science, 49(8), 817-830, doi:10.1016/S0032-
981 0633(01)00032-0.
982 Keller, G., 2003. Biotic effects of impacts and volcanism. Earth and Planetary Science
983 Letters, 215, 249-264, doi:10.1016/S0012-821X(03)00390-X.
984 Keller, G., 2011. Defining the Cretaceous-Tertiary boundary: a practical guide and return
985 to first principles. In: Keller, G., Adatte, T. (Eds.), The KT Mass Extinction and the
986 Chicxulub impact in Texas. SEPM Special Publication, 100, 23-42.
987 Keller, G., 2014. Deccan volcanism, the Chicxulub impact, and the end-Cretaceous mass
988 extinction: Coincidence? Cause and effect? In: Keller, G., Kerr, A. (Eds.),
989 Volcanism, Impacts and Mass Extinctions: Causes and Effects. Geological Society
990 of America Special Papers, 505, 57-89, doi:10.1130/2014.2505(03).
991 Keller, G., and Abramovich, S., 2009. Lilliput effect in late Maastrichtian planktic
992 foraminifera: Response to environmental stress. Palaeogeography,
993 Palaeoclimatology, Palaeoecology, 284, 47-62, doi:10.1016/j.palaeo.2009.08.029.
994 Keller, G., and Lindinger, M., 1989. Stable isotope, TOC and CaCO3 record across the
995 Cretaceous/Tertiary boundary at El Kef, Tunisia. Palaeogeography,
996 Palaeoclimatology, Palaeoecology, 73(3-4), 243-265, doi:10.1016/0031-
997 0182(89)90007-2.

998 Keller, G., Li, L., and MacLeod, N., 1995. The Cretaceous-Tertiary boundary stratotype
999 section at El Kef, Tunisia: how catastrophic was the mass extinction?
1000 Palaeogeography, Palaeoclimatology, Palaeoecology, 119, 221- 254,
1001 doi:10.1016/0031-0182(95)00009-7.
1002 Keller, G., Adatte, T., Stinnesbeck, W., Luciani, V., Karoui-Yaakoub, N., and Zaghbib-
1003 Turki, D., 2002. Paleoecology of the Cretaceous–Tertiary mass extinction in
1004 planktonic foraminifera. Palaeogeography, Palaeoclimatology, Palaeoecology,
1005 178(3), 257-297, doi:10.1016/S0031-0182(01)00399-6.
1006 Keller, G., Adatte, T., Tantawy, A.A., Berner, Z., and Stüben, D., 2007. High stress late
1007 Cretaceous to early Danian paleoenvironment in the Neuquen Basin, Argentina.
1008 Cretaceous Research, 28, 939-960, doi:10.1016/j.cretres.2007.01.006.
1009 Keller, G., Adatte, T., Gardin, S., Bartolini, A., and Bajpai, S., 2008. Main Deccan
1010 volcanism phase ends near the K-T boundary: evidence from the Krishna-Godavari
1011 Basin, SE India. Earth and Planetary Science Letters, 268, 293-311,
1012 doi:10.1016/j.epsl.2008.01.015.
1013 Keller, G., Adatte, T., Pardo, A., Lopez-Oliva, J.G., 2009. New evidence concerning the
1014 age and biotic effects of the Chicxulub impact in NE Mexico. Journal of the
1015 Geological Society of London, 166(3), 393-411, doi:10.1144/0016-76492008-116.
1016 Keller, G., Bhowmick, P.K., Upadhyay, H., Dave, A., Reddy, A.N., Jaiprakash, B.C., and
1017 Adatte, T., 2011a. Deccan volcanism linked to the Cretaceous-Tertiary boundary
1018 (KTB) mass extinction: New evidence from ONGC wells in the Krishna-Godavari
1019 Basin, India. Journal of the Geological Society of India, 78, 399-428,
1020 doi:10.1007/s12594-011-0107-3.

1021 Keller, G., Abramovich, S., Adatte, T., and Berner, Z., 2011b. Biostratigraphy, Age of
1022 the Chicxulub impact, and depositional environment of the Brazos River KTB
1023 sequences. In: Keller, G., Adatte, T. (Eds.), The End-Cretaceous Mass Extinction
1024 and the Chicxulub Impact in Texas. Society for Sedimentary Geology Special
1025 Publication 100, 81-122, doi:10.2110/sepmsp.100.081.
1026 Keller, G., Adatte, T., Bhowmick, P.K., Upadhyay, H., Dave, A., Reddy, A.N., and
1027 Jaiprakash, B.C., 2012. Nature and timing of extinctions in Cretaceous–Tertiary
1028 planktic foraminifera preserved in Deccan intertrappean sediments of the Krishna-
1029 Godavari Basin, India. Earth and Planetary Science Letters, 341, 211-221,
1030 doi:10.1016/j.epsl.2012.06.021.
1031 Keller, G., Khozyem, H.M., Adatte, T., Malarkodi, N., Spangenberg, J.E., and
1032 Stinnesbeck, W., 2013. Chicxulub impact spherules in the North Atlantic and
1033 Caribbean: age constraints and Cretaceous- Tertiary boundary hiatus. Geological
1034 Magazine, 150, 885-907, doi:10.1017/S0016756812001069.
1035 Keller, G., Punekar, J., and Mateo, P., 2016. Upheavals during the late Maastrichtian:
1036 Volcanism, climate and faunal events preceding the end-Cretaceous mass
1037 extinction. Palaeogeography, Palaeoclimatology, Palaeoecology, 441, 137-151,
1038 doi:10.1016/j.palaeo.2015.06.034.
1039 Kelly, D.C., Bralower, T.J., Zachos, J.C., Premoli-Silva, I., and Thomas, E., 1996. Rapid
1040 diversification of planktonic foraminifera in the tropical Pacific (ODP Site 865)
1041 during the late Paleocene Thermal Maximum. Geology, 24, 423-426, doi:
1042 10.1130/0091-7613(1996)024<0423:RDOPFI>2.3.CO;2.

1043 Kelly, D. C., Bralower, T. J., and Zachos, J. C., 1998. Evolutionary consequences of the
1044 latest Paleocene thermal maximum for tropical planktonic foraminifera.
1045 Palaeogeography, Palaeoclimatology, Palaeoecology, 141, 139-161,
1046 doi:10.1016/S0031-0182(98)00017-0.
1047 Kennett, J.P., and Stott, L.D., 1991. Abrupt deep-sea warming, palaeoceanographic
1048 changes and benthic extinctions at the end of the Palaeocene. Nature, 353, 225-229.
1049 Khozyem, H., Adatte, T., Keller, G., Tantawy, A.A., and Spangenberg, J.E., 2014. The
1050 Paleocene-Eocene GSSP at Dababiya, Egypt-Revisited. Episodes, 37(2), 78-86.
1051 Khozyem, H., Adatte, T., Spangenberg, J.E., Keller, G., Tantawy, A.A., and Ulianov, A.,
1052 2015. New geochemical constraints on the Paleocene–Eocene thermal maximum:
1053 Dababiya GSSP, Egypt. Palaeogeography, Palaeoclimatology, Palaeoecology, 429,
1054 117-135, doi:10.1016/j.palaeo.2015.04.003.
1055 Koch, P.L., Zachos, J.C., and Gingerich, P.D., 1992. Correlation between isotope records
1056 in marine and continental carbon reservoirs near the Palaeocene/Eocene boundary.
1057 Nature, 358(6384), 319-322, doi:10.1002/palo.20016.
1058 Koch, P.L., Zachos, J.C., and Dettman, D.L., 1995. Stable isotope stratigraphy and
1059 paleoclimatology of the Paleogene Bighorn Basin (Wyoming, USA).
1060 Palaeogeography, Palaeoclimatology, Palaeoecology, 115(1-4), 61-89,
1061 doi:10.1016/0031-0182(94)00107-J.
1062 Kump, L.R., 1991, Interpreting carbon-isotope excursions: strangelove oceans. Geology,
1063 19, 299-302, doi:10.1130/0091-7613(1991)019<0299:ICIESO>2.3.CO;2.

1064 Kump, L.R., 2003, The Geochemistry of Mass Extinction. In: Mackenzie, F.T. (Ed.)
1065 Treatise on Geochemistry, 7, Elsevier, 351-367, doi:10.1016/B0-08-043751-
1066 6/07101-2.
1067 Kump, L., Bralower, T., and Ridgwell, A., 2009. Ocean acidification in deep time.
1068 Oceanography, 22(4), 94-107.
1069 Labandeira, C.C., Johnson, K.R., and Lang, P., 2002. Preliminary assessment of insect
1070 herbivory across the Cretaceous-Tertiary boundary: major extinction and minimum
1071 rebound. Geological Society of America Special Paper 361, 297-327.
1072 Le Quéré, C., Andres, R.J., Boden, T., Conway, T., Houghton, R.A., House, J.I.,
1073 Marland, G., Peters, G.P., Van der Werf, G.R., Ahlström, A., and Andrew, R.M.,
1074 2013. The global carbon budget 1959–2011. Earth System Science Data, 5(1), 165-
1075 185, doi:10.5194/essd-5-165-2013.
1076 Leakey, R., and Lewin, R., 1992. The Sixth Extinction: Patterns of Life and the Future of
1077 Humankind. Anchor Books, pp. 271.
1078 Li, L., and Keller, G., 1998. Abrupt deep-sea warming at the end of the Cretaceous.
1079 Geology, 26, 995-998, doi:10.1130/0091-
1080 7613(1998)026<0995:ADSWAT>2.3.CO;2.
1081 Longrich, N.R., Tokaryk, T., and Field, D.J., 2011. Mass extinction of birds at the
1082 Cretaceous–Paleogene (K–Pg) boundary. Proceedings of the National Academy of
1083 Sciences, 108(37), 15253-15257, doi:10.1073/pnas.1110395108.
1084 Longrich, N.R., Bhullar, B.A.S., and Gauthier, J.A., 2012. Mass extinction of lizards and
1085 snakes at the Cretaceous–Paleogene boundary. Proceedings of the National
1086 Academy of Sciences, 109(52), 21396-21401, doi:10.1073/pnas.1211526110.

1087 Lu, G., and Keller, G., 1993. Climatic and oceanographic events across the Paleocene-
1088 Eocene Transition in the Antarctic Indian Ocean: Inference from planktic
1089 foraminifera. Marine Micropaleontology, 21, 101-142.
1090 Lu, G., and Keller, G., 1995a. Ecological stasis and saltation: Species richness change in
1091 planktic foraminifera during the late Paleocene to early Eocene, DSDP Site 577.
1092 Palaeogeography, Palaeoclimatology, Palaeoecology, 117, 211-227,
1093 doi:10.1016/0031-0182(94)00125-R.
1094 Lu, G., and Keller, G., 1995b. Planktic foraminiferal turnovers in the subtropical Pacific
1095 during the late Paleocene to early Eocene. Journal of Foraminiferal Research, 25:
1096 97-116.
1097 Lu, G., Keller, G, Adatte, T., Ortiz, N., and Molina, E., 1996. Long-term (10^5) or short-
1098 term (10^3) $\delta^{13}C$ excursion near the Paleocene-Eocene transition: evidence from the
1099 Tethys. Terra Nova, 8, 347-355.
1100 Lu, G., Adatte, T., Keller, G., and Ortiz, S., 1998. Abrupt climatic, oceanographic and
1101 ecologic changes near the Paleocene-Eocene transition in the deep Tethys basin: the
1102 Alamedilla section, southern Spain. Eclogae Geologicae Helvetiae, 91, 293-306.
1103 Luciani, V., 2002. High-resolution planktonic foraminiferal analysis from the
1104 Cretaceous–Tertiary boundary at Ain Settara (Tunisia): evidence of an extended
1105 mass extinction. Palaeogeography, Palaeoclimatology, Palaeoecology, 178(3), 299-
1106 319, doi:10.1016/S0031-0182(01)00400-X.
1107 Luciani, V., Giusberti, L., Agnini, C., Backman, J., Fornaciari, E., and Rio, D., 2007. The
1108 Paleocene-Eocene Thermal Maximum as recorded by Tethyan planktonic

1109 foraminifera in the Forada section (northern Italy). Marine Micropaleontology,
1110 64(3), 189-214, doi:10.1016/j.marmicro.2007.05.001.
1111 Luciani, V., Dickens, G.R., Backman, J., Fornaciari, E., Giusberti, L., Agnini, C., and
1112 D'Onofrio, R., 2016. Major perturbations in the global carbon cycle and
1113 photosymbiont-bearing planktic foraminifera during the early Eocene. Climate of
1114 the past, 12, 981-1007, doi:10.5194/cp-12-981-2016.
1115 Maclennan, J. and Jones, S.M., 2006. Regional uplift, gas-hydrate dissociation and the
1116 origins of the Paleocene–Eocene Thermal Maximum. Earth and Planetary Science
1117 Letters, 245(1), 65-80, doi: 10.1016/j.epsl.2006.01.069.
1118 MacLeod, N., Rawson, P.F., Forey, P.L., Banner, F.T., Boudagher-Fadel, M.K., Bown,
1119 P.R., Burnett, J.A., Chambers, P., Culver, S., Evans, S.E., Jeffery, C., Kaminski,
1120 M.A., Lord, A.R., Milner, A.C., Milner, A.R., Morris, N., Owen, E., Rosen, B.R.,
1121 Smith, A.B., Taylor, P.D., Urquhart, E., and Young, J.R., 1997. The Cretaceous-
1122 tertiary biotic transition. Journal of the Geological Society, 154(2), 265-292, doi:
1123 10.1144/gsjgs.154.2.0265.
1124 Mateo, P., Keller, G., Punekar, J., and Spangenberg, J.E., 2017. Early to Late
1125 Maastrichtian environmental changes in the Indian Ocean compared with Tethys
1126 and South Atlantic. Palaeogeography, Palaeoclimatology, Palaeoecology, 478, 121-
1127 138, doi:10.1016/j.palaeo.2017.01.027.
1128 May, R.M., Lawton, J.H., and Stork, N.E., 1995. Assessing extinction rates. Extinction
1129 rates, 1-24.
1130 McInerney, F.A., and Wing, S.L., 2011. The Paleocene-Eocene Thermal Maximum: a
1131 perturbation of carbon cycle, climate, and biosphere with implications for the

1132 future. Annual Review of Earth and Planetary Sciences, 39, 489-516,
1133 doi:10.1146/annurev-earth-040610-133431.
1134 McNeil, B.I., and Matear, R.J., 2008. Southern Ocean acidification: A tipping point at
1135 450-ppm atmospheric CO2. Proceedings of the National Academy of Sciences,
1136 105(48), 18860-18864.doi:10.1073/pnas.0806318105.
1137 Molina, E., Arenillas, I., and Arz, J.A., 1998. Mass extinction in planktic foraminifera at
1138 the Cretaceous/Tertiary boundary in subtropical and temperate latitudes. Bulletin de
1139 la Société géologique de France, 169(3), 351-363.
1140 Molina, E., Alegret, L., Arenillas, I., Arz, J.A., Gallala, N., Hardenbol, J., von Salis, K.,
1141 Steurbaut, E., Vandenberghe, N., and Zaghbib-Turki, D., 2006. The Global
1142 Boundary Stratotype Section and Point for the base of the Danian Stage (Paleocene,
1143 Paleogene, “Tertiary”, Cenozoic) at El Kef, Tunisia: Original definition and
1144 revision. Episodes, 29(4), 263-273.
1145 Molina, E., Alegret, L., Arenillas, I., Arz, J.A., Gallala, N., Grajales-Nishimura, J.M.,
1146 Murillo-Muneton, G., and Zaghbib-Turki, D., 2009. The Global Boundary
1147 Stratotype Section and Point for the Base of the Danian Stage (Paleocene,
1148 Paleogene," Tertiary", Cenozoic): Auxiliary Sections and Correlation. Episodes,
1149 32(2), 84-95.
1150 Nichols, D.J., and Johnson, K.R., 2008. Plants and the KT Boundary. Cambridge
1151 University Press, New York, p. 279.
1152 Nordt, L., Atchley, S., and Dworkin, S., 2003. Terrestrial evidence for two greenhouse
1153 events in the Latest Cretaceous. GSA Today 13, 4-9.

1154 Olsson, R.K., Hemleben, C., Berggren, W.A., and Huber, B.T., 1999. Atlas of Paleocene
1155 Planktonic Foraminifera. Smithsonian Contributions to Paleobiology, 85.
1156 Washington, DC, Smithsonian Institution Press, pp. 252.
1157 Olsson, R.K., Wright, J.D., and Miller, K.G., 2001. Paleobiogeography of
1158 *Pseudotextularia elegans* during the latest Maastrichtian global warming event.
1159 Journal of Foraminiferal Research, 31, 275-282, doi:10.2113/31.3.275.
1160 Panchuk, K., Ridgwell, A. and Kump, L.R., 2008. Sedimentary response to Paleocene-
1161 Eocene Thermal Maximum carbon release: A model-data comparison. Geology,
1162 36(4), 315-318, doi: 10.1130/G24474A.1.
1163 Pardo, A., and Keller, G., 2008. Biotic effects of environmental catastrophes at the end of
1164 the Cretaceous: Guembelitria and Heterohelix blooms. Cretaceous Research, 29(5-
1165 6), 1058-1073, doi:10.1016/j.cretres.2008.05.031.
1166 Pardo, A., Ortiz, N., and Keller, G., 1996. Latest Maastrichtian and K/T boundary
1167 foraminiferal turnover and environmental changes at Agost, Spain. In: MacLeod,
1168 N., Keller, G. (Eds.), The Cretaceous-Tertiary Mass Extinction: Biotic and
1169 Environmental Effects. New York, Norton Press, 157-191.
1170 Pardo, A., Keller, G., and Oberhaensli, H., 1999. Paleoecologic and paleoceanographic
1171 evolution of the Tethyan realm during the Paleocene-Eocene transition. Journal of
1172 Foraminiferal Research, 29(1), 37-57.
1173 Payne, J.L., 2005. Evolutionary dynamics of gastropod size across the end-Permian
1174 extinction and through the Triassic recovery interval. Paleobiology, 31(2), 269-290,
1175 doi:10.1666/0094-8373(2005)031[0269:EDOGSA]2.0.CO;2.

1176 Pearson, P.N., Olsson, R.K., Huber, B.T., Hemleben, C., and Berggren, W.A., 2006.
1177 Atlas of Eocene planktonic foraminifera 41. Cushman Foundation Special
1178 Publication, 1-513.
1179 Penman, D.E., Hönisch, B., Zeebe, R.E., Thomas, E. and Zachos, J.C., 2014. Rapid and
1180 sustained surface ocean acidification during the Paleocene-Eocene Thermal
1181 Maximum. Paleoceanography, 29(5), 357-369, doi: 10.1002/2014PA002621.
1182 Percival, L.M.E., Witt, M.L.I., Mather, T.A., Hermoso, M., Jenkyns, H.C., Hesselbo,
1183 S.P., Al-Suwaidi, A.H., Storm, M.S., Xu, W., and Ruhl, M., 2015. Globally
1184 enhanced mercury deposition during the end-Pliensbachian extinction and Toarcian
1185 OAE: A link tothe Karoo–Ferrar large igneous province. Earth and Planetary
1186 Science Letters, 428, 267-280, doi:10.1016/j.epsl.2015.06.064.
1187 Pereira, H.M., Leadley, P.W., Proença, V., Alkemade, R., Scharlemann, J.P., Fernandez-
1188 Manjarrés, J.F., Araújo, M.B., Balvanera, P., Biggs, R., Cheung, W.W., and Chini,
1189 L., 2010. Scenarios for global biodiversity in the 21st century. Science, 330(6010),
1190 1496-1501, doi:10.1126/science.1196624.
1191 Punekar, J., and Saraswati, P.K., 2010. Age of the Vastan lignite in context of some
1192 oldest Cenozoic fossil mammals from India. Journal of the Geological Society of
1193 India, 76(1), 63-68, doi:10.1007/s12594-010-0076-y.
1194 Punekar, J., Mateo, P., and Keller, G., 2014. Effects of Deccan volcanism on
1195 paleoenvironment and planktic foraminifera: A global survey. Geological Society
1196 of America Special Papers, 505, 91-116, doi: 10.1130/2014.2505(04).
1197 Punekar, J., Keller, G., Khozyem, H. M., Adatte, T., Font, E., and Spangenberg, J., 2016.
1198 A multi-proxy approach to decode the end-Cretaceous mass extinction.

1199 Palaeogeography, Palaeoclimatology, Palaeoecology, 441, 116-136,
1200 doi:10.1016/j.palaeo.2015.08.025.
1201 Remane, J., Keller, G., Hardenbol, J., and Ben Haj Ali, M., l999. Report on the
1202 International Workshop on Cretaceous-Paleogene Transitions. Episodes, 22, 47-48.
1203 Renne, P.R., Sprain, C.J., Richards, M.A., Self, S., Vanderkluysen, L., and Pande, K.,
1204 2015. State shift in Deccan volcanism at the Cretaceous-Paleogene boundary,
1205 possibly induced by impact. Science, 350(6256), 76-78,
1206 doi:10.1126/science.aac7549.
1207 Richards, M.A., Alvarez, W., Self, S., Karlstrom, L., Renne, P.R., Manga, M., Sprain,
1208 C.J., Smit, J., Vanderkluysen, L., and Gibson, S.A., 2015. Triggering of the largest
1209 Deccan eruptions by the Chicxulub impact. Geological Society of America Bulletin,
1210 127(11-12), 1507-1520, doi:10.1130/B31167.1.
1211 Rose, K.D., DeLeon, V.B., Missiaen, P., Rana, R.S., Sahni, A., Singh, L., and Smith, T.,
1212 2008. Early Eocene lagomorph (Mammalia) from Western India and the early
1213 diversification of Lagomorpha. Proceedings of the Royal Society of London B:
1214 Biological Sciences, 275(1639), 1203-1208, doi:10.1098/rspb.2007.1661.
1215 Schoene, B., Samperton, K.M., Eddy, M.P., Keller, G., Adatte, T., Bowring, S.A.,
1216 Khadri, S.F.R., and Gertsch, B., 2015. U–Pb geochronology of the Deccan Traps
1217 and relation to the end-Cretaceous mass extinction. Science, 347, 182-184,
1218 doi:10.1126/science.aaa0118.
1219 Schulte, P., Alegret, L., Arenillas, I., Arz, J.A., Barton, P.J., Bown, P.R., Bralower, T.J.,
1220 Christeson, G.L., Claeys, P., Cockell, C.S., Collins, G.S., Deutsch, A., Goldin, T.J.,
1221 Goto, K., Grajales-Nishimura, J.M., Grieve, R.A.F., Gulick, S.P.S., Johnson, K.R.,

Kiessling, W., Koeberl, C., Kring, D.A., MacLeod, K.G., Matsui, T., Melosh, J., Montanari, A., Morgan, J.V., Neal, C.R., Nichols, D.J., Norris, R.D., Pierazzo, E., Ravizza, G., Rebolledo-Vieyra, M., Reimold, W.U., Robin, E., Salge, T., Speijer, R.P., Sweet, A.R., Urrutia-Fucugauchi, J., Vajda, V., Whalen, M.T., and Willumsen, P.S., 2010. The Chicxulub asteroid impact and mass extinction at the Cretaceous-Paleogene boundary. Science, 327, 1214-1218, doi:10.1126/science.1177265.

Schulte, P., Scheibner, C., and Speijer, R., 2011. Fluvial discharge and sea-level changes controlling black shale deposition during the Paleocene–Eocene Thermal Maximum in the Dababiya Quarry section, Egypt. Chemical Geology, 285, 167-183, doi:10.1016/j.chemgeo.2011.04.004.

Scotese, C.R., 2013a. Map Folio 16, KT Boundary (65.5 Ma, latest Maastrichtian), PALEOMAP PaleoAtlas for ArcGIS, volume 2, Cretaceous, PALEOMAP Project, Evanston, IL, doi:10.13140/2.1.3498.1129.

Scotese, C.R., 2013b. Map Folio 14, PETM (55.8 Ma, Thanetian/Ypresian Boundary), PALEOMAP PaleoAtlas for ArcGIS, volume 1, Cenozoic, PALEOMAP Project, Evanston, IL, doi:10.13140/2.1.2388.0961.

Self, S., Jay, A.E., Widdowson, M., and Keszthelyi, L.P., 2008. Correlation of the Deccan and Rajahmundry Trap lavas: Are these the longest and largest lava flows on Earth? Journal of Volcanology and Geothermal Research, 172, 3-19, doi:10.1016/j.jvolgeores.2006.11.012.

Self, S., Schmidt, A., and Mather, T.A., 2014. Emplacement characteristics, time scales, and volcanic gas release rates of continental flood basalt eruptions on Earth. In:

Keller, G., Kerr, A.C. (Eds.), Volcanism, Impacts, and Mass Extinctions: Causes and Effects. Geological Society of America Special Paper 505, 319-337, doi:10.1130/2014.2505(16).

Sigurdsson, H., Leckie, R.M., and Acton, G., 1997. Proceedings of the Ocean Drilling Program, Initial reports, Volume 165. College Station, Texas, Ocean Drilling Program, 865 p.

Silva, M.V.N., Sial, N.A., Barbosa, J.A., Ferreira, V.P., Neumann, V.H., and de Lacerca, L.D., 2013. Carbon isotopes, rare-earth elements and mercury geochemistry across the K-T transition of the Paraíba Basin, northeastern Brazil. Geological Society of London Special Publication 382, 85-104, doi:10.1144/SP382.2.

Sinton, C.W., and Duncan, R.A., 1998. ^{40}Ar-^{39}Ar ages of lavas from the Southeast Greenland margin, ODP Leg 152, and the Rockall Plateau, DSDP Leg 81. Proceedings of the Ocean Drilling Program, Scientific Results, 152, 387-402, doi:10.2973/odp.proc.sr.152.234.1998.

Sluijs, A., Schouten, S., Pagani, M., Woltering, M., Brinkhuis, H., Damsté, J.S.S., Dickens, G.R., Huber, M., Reichart, G-J, Stein, R., Matthiessen, J., Lourens, L.J., Pedentchouk, N., Backman, J., Moran, K., and the Expedition 302 Scientists, 2006. Subtropical Arctic Ocean temperatures during the Palaeocene/Eocene thermal maximum. Nature, 441(7093), 610-613, doi:10.1038/nature04668.

Sluijs, A., Brinkhuis, H., Crouch, E.M., John, C.M., Handley, L., Munsterman, D., Bohaty, S.M., Zachos, J.C., Reichart, G.-J., Schouten, S., Pancost, R.D., and Sinninghe Damste, J.S., 2008. Eustatic variations in the Paleocene–Eocene greenhouse world. Paleoceanography, 23, PA4216, doi:10.1029/2008PA001615.

1268 Smith, F.A., 2012. Some like it hot. Science, 335(6071), 924-925,
1269 doi:10.1126/science.1219233.
1270 Smith, T., Rose, K.D., and Gingerich, P.D., 2006. Rapid Asia–Europe–North America
1271 geographic dispersal of earliest Eocene primate Teilhardina during the Paleocene–
1272 Eocene thermal maximum. Proceedings of the National Academy of Sciences,
1273 103(30), 11223-11227, doi:10.1073/pnas.0511296103.
1274 Smith, J.J., Hasiotis, S.T., Kraus, M.J., and Woody, D.T., 2009. Transient dwarfism of
1275 soil fauna during the Paleocene–Eocene Thermal Maximum. Proceedings of the
1276 National Academy of Sciences, 106(42), 17655-17660,
1277 doi:10.1073/pnas.0909674106.
1278 Soliman, M.F., Ahmed, E., and Kurzweil, H., 2006. Geochemistry and mineralogy of the
1279 Paleocene/Eocene boundary at Gabal Dababiya (GSSP) and Gabal Owaina sections,
1280 Nile Valley, Egypt. Stratigraphy, 3, 31-52.
1281 Speijer, R.P. and Schmitz, B., 1998. A benthic foraminiferal record of Paleocene sea
1282 level and trophic/redox conditions at Gebel Aweina, Egypt. Palaeogeography,
1283 Palaeoclimatology, Palaeoecology, 137, 79-101, doi:10.1016/S0031-
1284 0182(97)00107-7.
1285 Speijer, R.P., and Van der Zwaan, G.J., 1996. Extinction and survivorship of southern
1286 Tethyan benthic foraminifera across the Cretaceous/Palaeogene boundary.
1287 Geological Society of London Special Publications, 102(1), 343-371, doi:
1288 10.1144/GSL.SP.1996.001.01.26.
1289 Speijer, R.P., and Wagner, T., 2002. Sea-level changes and black shales associated with
1290 the late Paleocene thermal maximum: Organic-geochemical and micropaleontologic

1291 evidence from the southern Tethyan margin (Egypt-Israel). Geological Society of
1292 America Special Paper, 356, 533-549.
1293 Speijer, R.P., Schmitz, B., Aubry, M.P. and Charisi, S.D., 1995. The latest Paleocene
1294 benthic extinction event: punctuated turnover in outer neritic foraminiferal faunas
1295 from Gebel Aweina, Egypt. Israel Journal of Earth Sciences, 44, 207-222.
1296 Storey, M., Duncan, R.A., and Swisher, C.C., 2007. Paleocene-Eocene Thermal
1297 Maximum and the opening of the northeast Atlantic. Science, 316, 587, doi:
1298 10.1126/science.1135274.
1299 Stüben, D., Kramar, U., Berner, Z.A., Meudt, M., Keller, G., Abramovich, S., Adatte, T.,
1300 Hambach, U., and Stinnesbeck, W., 2003. Late Maastrichtian paleoclimatic and
1301 paleoceanographic changes inferred from Sr/Ca ratio and stable isotopes.
1302 Paleoclimatology, Paleoecology, Paleogeography 199, 107-127,
1303 doi:10.1016/S0031-0182(03)00499-1.
1304 Sunday, J.M., Calosi, P., Dupont, S., Munday, P.L., Stillman, J.H., and Reusch, T.B.,
1305 2014. Evolution in an acidifying ocean. Trends in Ecology & Evolution, 29(2), 117-
1306 125, doi:10.1016/j.tree.2013.11.001.
1307 Svensen, Henrik, Sverre Planke, Anders Malthe-Sørenssen, Bjørn Jamtveit, Reidun
1308 Myklebust, Torfinn Rasmussen Eidem, and Sebastian S. Rey, 2004. Release of
1309 methane from a volcanic basin as a mechanism for initial Eocene global warming.
1310 Nature, 429, 6991, 542-545, doi:10.1038/nature02566.
1311 Svensen, H., Planke, S., and Corfu, F., 2010. Zircon dating ties NE Atlantic sill
1312 emplacement to initial Eocene global warming. Journal of the Geological Society of
1313 London, 167, 433-436, doi: 10.1144/0016-76492009-125.

1314 Thibault, N., and Husson, D., 2016. Climatic fluctuations and sea-surface water
1315 circulation patterns at the end of the Cretaceous era: Calcareous nannofossil
1316 evidence. Palaeogeography, Palaeoclimatology, Palaeoecology, 441, 152-164,
1317 doi:10.1016/j.palaeo.2015.07.049.
1318 Thibault, N., Galbrun, B., Gardin, S., Minoletti, F., and Le Callonec, L., 2016. The end-
1319 Cretaceous in the southwestern Tethys (Elles, Tunisia): orbital calibration of
1320 paleoenvironmental events before the mass extinction. International Journal of
1321 Earth Sciences, 1-25, doi:10.1007/s00531-015-1192-0.
1322 Thibodeau, A.M., and Bergquist, B.A., 2017. Do mercury isotopes record the signature of
1323 massive volcanism in marine sedimentary records? Geology, 45(1), 95-96,
1324 doi:10.1130/focus012017.1.
1325 Thibodeau, A.M., Ritterbush, K., Yager, J.A., West, A.J., Ibarra, Y., Bottjer, D.J.,
1326 Berelson, W.M., Bergquist, B.A., and Corsetti, F.A, 2016. Mercury anomalies and
1327 the timing of biotic recovery following the end-Triassic mass extinction. Nature
1328 communications, 7, doi:10.1038/ncomms11147.
1329 Twitchett, R.J., 2007. The Lilliput effect in the aftermath of the end-Permian extinction
1330 event. Palaeogeography, Palaeoclimatology, Palaeoecology, 252(1), 132-144,
1331 doi:10.1016/j.palaeo.2006.11.038.
1332 Thomas, E., 1998. The biogeography of the late Paleocene benthic foraminiferal
1333 extinction. In: Aubry, M.-P., Lucas, S., and Berggren, W.A. (Eds.), Late Paleocene–
1334 Early Eocene Biotic and Climatic Events in the Marine and Terrestrial Records.
1335 University Press, Columbia, pp. 214-243.

1336 Tong, Y., and Wang, J., 2006. Fossil mammals from the early Eocene Wutu formation of
1337 Shandong province. Palaeontologia Sinica, new series C, 28, 1-195.
1338 Urbanek, A., 1993. Biotic crises in the history of Upper Silurian graptoloids: a
1339 palaeobiological model. Historical Biology, 7, 29-50.
1340 Vajda, V., and Bercovici, A., 2014. The global vegetation pattern across the Cretaceous–
1341 Paleogene mass extinction interval: A template for other extinction events. Global
1342 and Planetary Change, 122, 29-49, doi:10.1016/j.gloplacha.2014.07.014.
1343 Wake, D.B., and Vredenburg, V.T., 2008. Are we in the midst of the sixth mass
1344 extinction? A view from the world of amphibians. Proceedings of the National
1345 Academy of Sciences, 105(1), 11466-11473.
1346 Weijers, J.W., Schouten, S., Sluijs, A., Brinkhuis, H., and Damsté, J.S.S., 2007. Warm
1347 arctic continents during the Palaeocene–Eocene thermal maximum. Earth and
1348 Planetary Science Letters, 261(1), 230-238, doi:10.1016/j.epsl.2007.06.033.
1349 Westerhold, T., Röhl, U., McCarren, H.K., and Zachos, J.C., 2009. Latest on the absolute
1350 age of the Paleocene–Eocene Thermal Maximum (PETM): new insights from exact
1351 stratigraphic position of key ash layers+ 19 and− 17. Earth and Planetary Science
1352 Letters, 287(3), 412-419, doi:10.1016/j.epsl.2009.08.027.
1353 Westerhold, T., Röhl, U., Donner, B., McCarren, H.K., and Zachos, J.C., 2011. A
1354 complete high-resolution Paleocene benthic stable isotope record for the central
1355 Pacific (ODP Site 1209). Paleoceanography, 26, PA2216,
1356 doi:10.1029/2010PA002092.
1357 Whalen, M.T., Day, J., Eberli, G.P., and Homewood, P.W., 2002. Microbial carbonates
1358 as indicators of environmental change and biotic crisis in carbonate systems:

examples from the Late Devonian, Alberta Basin, Canada. Palaeogeography, Palaeoclimatology, Palaeoecology, 181, 127-151.

Wieczorek, R., Fantle, M.S., Kump, L.R., and Ravizza, G., 2013. Geochemical evidence for volcanic activity prior to and enhanced terrestrial weathering during the Paleocene Eocene Thermal Maximum. Geochimica et Cosmochimica Acta, 119, 391-410, doi:10.1016/j.gca.2013.06.005.

Wilf, P., and Johnson, K.R., 2004. Land plant extinction at the end of the Cretaceous: a quantitative analysis of the North Dakota megafloral record. Paleobiology, 30(3), 347-368, doi:10.1666/0094-8373(2004)030<0347:LPEATE>2.0.CO;2.

Wilf, P., Johnson, K.R., and Huber, B.T., 2003. Correlated terrestrial and marine evidence for global climate changes before mass extinction at the Cretaceous-Paleogene boundary. Proceedings of the National Academy of Sciences of the United States of America, 100(2), 599-604, doi:10.1073/pnas.0234701100.

Wilson, G.P., 2014. Mammalian extinction, survival, and recovery dynamics across the Cretaceous-Paleogene boundary in northeastern Montana, USA. Geological Society of America Special Papers, 503, 365-392, doi:10.1130/2014.2503(15).

Wilson, G.P., 2005. Mammalian faunal dynamics during the last 1.8 million years of the Cretaceous in Garfield County, Montana. Journal of Mammalian Evolution, 12(1-2), 53-76, doi:10.1007/s10914-005-6943-4.

Wilson, G.P., DeMar, D.G., and Carter, G., 2014. Extinction and survival of salamander and salamander-like amphibians across the Cretaceous-Paleogene boundary in northeastern Montana, USA. Geological Society of America Special Papers, 503, 271-297, doi:10.1130/2014.2503(10).

1382 Zachos, J., Arthur, M., and Dean, W., 1989. Geochemical evidence for suppression of
1383 pelagic marine productivity at the Cretaceous/Tertiary boundary. Nature, 337, 61-
1384 64, doi:10.1038/337061a0.
1385 Zachos, J.C., Wara, M.W., Bohaty, S., Delaney, M.L., Petrizzo, M.R., Brill, A.,
1386 Bralower, T.J., and Premoli Silva, I., 2003. A transient rise in tropical sea surface
1387 temperature during the Paleocene–Eocene Thermal Maximum. Science, 302, 1551-
1388 1554, doi: 10.1126/science.1090110.
1389 Zachos, J.C., Röhl, U., Schellenberg, S.A., Sluijs, A., Hodell, D.A., Kelly, D.C., Thomas,
1390 E., Nicolo, M., Raffi, I., Lourens, L.J., McCarren, H., and Kroon, D., 2005. Rapid
1391 acidification of the ocean during the Paleocene–Eocene Thermal Maximum.
1392 Science, 308, 1611-1615, doi:10.1126/science.1109004.
1393 Zachos, J.C., Schouten, S., Bohaty, S., Quattlebaum, T., Sluijs, A., Brinkhuis, H., Gibbs,
1394 S.J., and Bralower, T.J., 2006. Extreme warming of mid-latitude coastal ocean
1395 during the Paleocene-Eocene Thermal Maximum: Inferences from TEX86 and
1396 isotope data. Geology, 34(9), 737-740, doi:10.1130/G22522.1.
1397 Zachos, J.C., Dickens, G.R., and Zeebe, R.E., 2008. An early Cenozoic perspective on
1398 greenhouse warming and carbon-cycle dynamics. Nature, 451, 279-283,
1399 doi:10.1038/nature.
1400 Zeebe, R.E., 2012. History of seawater carbonate chemistry, atmospheric CO2, and ocean
1401 acidification. Annual Review of Earth and Planetary Sciences, 40, 141-165, doi:
1402 10.1146/annurev-earth-042711-105521.

1403 Zeebe, R.E., Zachos, J.C., and Dickens, G.R., 2009. Carbon dioxide forcing alone
1404 insufficient to explain Palaeocene–Eocene Thermal Maximum warming. Nature
1405 Geoscience, 2, 576-580, doi:10.1038/ngeo578.
1406

FIGURE CAPTIONS

Figure 1: (A) Paleogeography at the KPB (66.02 Ma) and paleolocations of El Kef and Elles sections, Reunion hotspot, Deccan volcanism and Chicxulub impact site. (B) Paleogeography at the PEB (55.8 Ma) and paleolocations of the Dababiya section, North Atlantic Igneous Province and circum-Caribbean volcanism. Paleomaps from Scotese (2013a, b).

Figure 2: Locations of the Cretaceous-Paleogene boundary (KPB) GSSP El Kef and Elles, Tunisia, and the Paleocene-Eocene boundary (PEB) GSSP at Dababiya, Egypt.

Figure 3: (A) The KPB event at Elles, Tunisia, is well exposed across the hillside marked by a lithological change from gray shale of the Maastrichtian to dark gray clay of the early Danian weathered to a light brownish color. (B) A 1-2 cm thick rusty "red layer" at the base of the KPB clay layer contains maximum Ir concentrations and marks the mass extinction. (C) A blow-up of this red layer shows the sharp contact with the Maastrichtian marl below and dark Danian clay of zone P0 above.

Figure 4: KPB extinction pattern at El Kef, Tunisia, shows all large tropical to subtropical species extinct at or near the KPB (2/3 of all species, SEM illustrations 1-10, numbers keyed to species), the short-term survivorship of small ecologically more tolerant species (1/3 of the species, SEMs 11-18) including a single long-term survivor (*Guembelitria cretacea*, SEM 14). Early Danian evolution begins within a few thousand

1430 years of the mass extinction but diversity remains low and species small (SEMs 1-9)
1431 marking high-stress conditions over ~500 ky of the earliest Danian. SEM illustrations are
1432 shown in relative species sizes in the assemblages. Faunal data updated from Keller
1433 (1988a).
1434
1435 **Figure 5:** El Kef, Tunisia, relative abundances of planktic foraminifera across the KPB
1436 (>63 μm size fraction for all species except 38-63 μm for *Guembelitria*) with SEM
1437 illustrations of marker species (numbers keyed to species names and abundance data).
1438 Carbon stable isotopes of bulk rock and benthic species *Anomalinoides acutus* across the
1439 KPB transition. Note the abrupt diversity change that marks the KPB mass extinction and
1440 the $\delta^{13}C$ negative shift that signals the collapse of primary productivity. Faunal data from
1441 Keller (1988a, updated), isotope data from Keller and Lindinger (1989).
1442
1443 **Figure 6:** (A) Relative abundances of planktic foraminifera (>63 μm) across the KPB at
1444 Elles, Tunisia, reveal low diversity assemblages dominated by small biserial species, but
1445 not *Guembelitria*, during the climate warming of the latest Maastrichtian and an interval
1446 of the early Danian. (B) Relative abundances of planktic foraminifera in the smaller (38-
1447 63 μm) size fraction reveals abundant dwarfed species in the earliest Danian as well as
1448 peak abundances (40 %) during the latest Maastrichtian preceding the mass extinction.
1449 This indicates that dwarfing of the disaster opportunist *Guembelitria* is a response to
1450 extreme environmental stress. SEM illustrations (numbers keyed to species names) are
1451 shown in relative species sizes in the assemblages. Faunal data from Keller et al. (2002).
1452

Figure 7: Effects of increasing environmental stress upon planktic foraminiferal assemblages from optimum to catastrophe conditions. Note the successive elimination of large, specialized k-strategy species during climate warming, particularly in restricted basins and marginal marine environments, and the survival of small r-strategy species commonly associated with volcanic activity. Disaster opportunists flood the environment during catastrophes. Modified from Keller and Abramovich (2009).

Figure 8: Early Danian evolution and decline in Cretaceous survivor species illustrate high-stress environments. Small dwarfed species and low diversity mark delayed marine recovery in magnetochron C29r from zones P0 through P1a(2) correlative with decreasing abundance and gradual extinction of dwarfed survivor species. The last phase of Deccan volcanism began near the zone P1a/P1b boundary (C29r/C29n) and marks the extinction of two dominant zone P1a index species (*Parvularugoglobigerina eugubina*, *P. longiapertura*). Marine recovery begins after this last volcanic phase and is marked by higher diversity and increasing species sizes. Note the number of the same specimens in each column indicates relative abundance. From Punekar et al. (2014).

Figure 9: Relative abundances of benthic foraminifera (>63 μm) and carbon stable isotopes of bulk rock and benthic species *Anomalinoides acutus* across the KPB transition at El Kef, Tunisia. Note the major faunal turnover across the KPB with up to 48 % species disappearing over 500 ky with many of them reappearing after environmental recovery. Faunal data from Keller (1988b); stable isotope data from Keller and Lindinger (1989).

Figure 10: Paleoenvironmental proxies (oxygen isotopes, mercury and disaster opportunist species) across the KPB at Elles, Tunisia. Note climate warming during the last 10 ky of the Maastrichtian coincides with increased Deccan volcanism (Hg/TOC ratio), which accelerates during the last thousand years and culminates with the KPB mass extinction. Hg and TOC data in Supplementary Materials S2, Table S2.

Figure 11: Paleoenvironmental proxies for the KPB transition at El Kef, Tunisia. The interval analyzed spans part of the latest Maastrichtian warming (zone CF1) marked by ocean acidification and high dissolution effects (FI), and 500 ky of the early Danian zones P0-P1a(2) marked by continuous high-stress low oxygen conditions and ends with the onset of recovery in P1b (base C29n). Data table (Table S1) in Supplementary Materials S2.

Figure 12: (A) Dababiya outcrop with GSSP designated cliff to the right and our sampled location 25 m to the left (East). (B) Sampling of the section using a ladder. (C) Contiguous outcrop between the GSSP cliff and our sampled section at 25 m east permits tracing the lithology bed by bed. Note the GSSP outcrop collapsed in the spring of 2016 at the vertical crack seen in C across the label "PEB". Armed guards protected the outcrop from eagerly sampling geologists.

Figure 13: (A) Relative abundances of planktic foraminifera, carbon stable isotopes and species richness at Dababiya, Egypt, 25 m east of the GSSP outcrop. The PETM interval

spans from its gradual onset 75 cm below to 1 m above the PEB and is marked by near total carbonate dissolution. Another strong dissolution interval at the base of the section has common benthic species but only rare planktics. Faunal data from this study, isotope data from Khozyem et al. (2014, 2015). (B) Relative abundances of benthic foraminifera show a major faunal turnover but few species extinctions (18 %, 7 species). Faunal data from Alegret and Ortiz (2006).

Figure 14: Paleoenvironmental proxies for the PETM transition at Dababiya, Egypt. Dissolution first appears in zone P4C coincident with high Hg/TOC values. The onset of the PETM begins with gradually decreasing $\delta^{13}C$ values in zone P5 that reached maximum at the PEB. Near total $CaCO_3$ dissolution in the lower part of zone E1 and strong dissolution in the upper part marks an interval nearly devoid of marine calcareous plankton during the PETM and signals strong ocean acidification despite the onset of recovery in $\delta^{13}C$ and $CaCO_3$. Faunal recovery begins in zone E2 with increasing $\delta^{13}C$ values and $CaCO_3$ reaching 60 %. Data table (Table S3) in Supplementary Materials S2.

Figure 15: Illustration of the KPB mass extinction, the PETM and Anthropocene climate warming. (A) During the latest Maastrichtian environmental devastation is mainly due to volcanism (ash, aerosols and greenhouse gases), resulting in rapid climate changes, acid rains and ocean acidification that is exacerbated by the Chicxulub impact, thus impeding calcification by marine plankton at the base of the food chain. (**B**) During the latest Paleocene to early Eocene: Gradual climate warming preceding the PEB is attributed to North Atlantic Igneous Province volcanism (NAIP), but the rapid warming of 5 °C

(PETM) is linked to methane hydrates released from continental shelves resulting in acid rain on land and ocean acidification (~170 ky). (**C**) During the Anthropocene large inputs of greenhouse gases (CO_2, SO_2, N_2O) linked to human activities and fossil fuel burning leads to rapid warming and ocean acidification at a rate exceeding those at the PETM and KPB by orders of magnitude. Global carbon budget data for the Anthropocene from Le Quéré et al. (2013). Illustration modified from Glikson (2014).

TABLE CAPTIONS

Table 1: Comparison of KPB, PETM and Anthropocene events based on climate and environmental changes shows great similarities, except that the Anthropocene warming is orders of magnitude more rapid than the PETM and KPB warming. The rate of faunal turnover and particularly extinctions is very difficult to estimate and contains the largest potential errors. At the current rate of CO_2 input into the atmosphere, the Anthropocene extinction is estimated to reach the 75 % mass extinction level within the next 250-500 ky.

***Graphical Abstract**

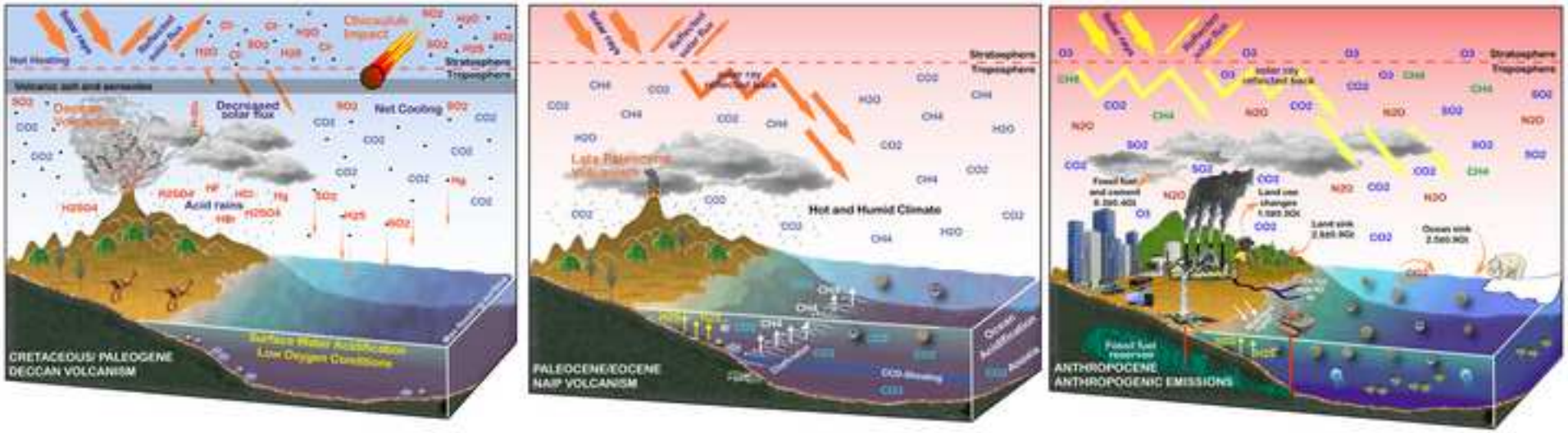

Figure 1

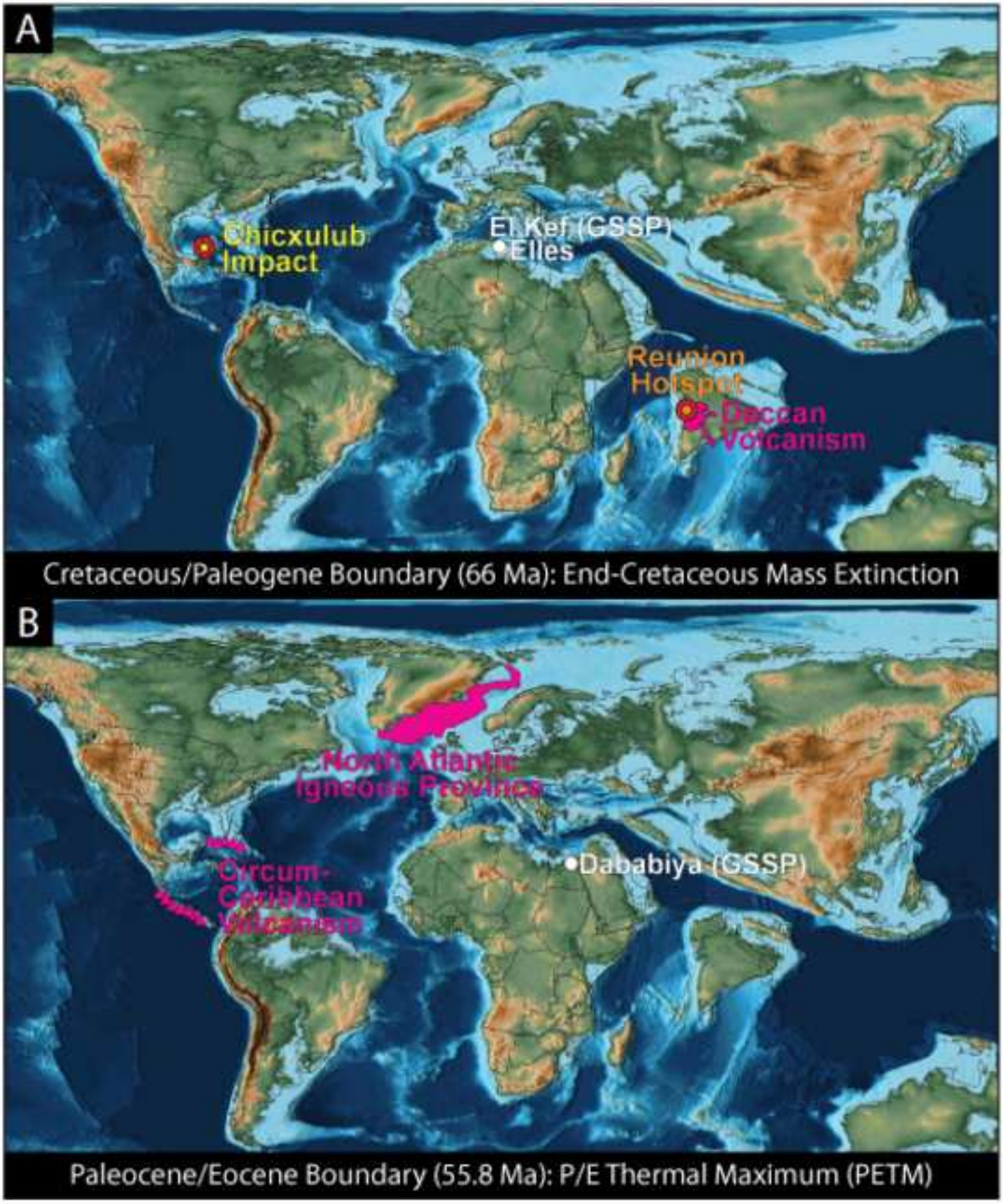
A
Chicxulub Impact
El Kef (GSSP)
Elles
Reunion Hotspot
Deccan Volcanism
Cretaceous/Paleogene Boundary (66 Ma): End-Cretaceous Mass Extinction
B
North Atlantic Igneous Provinces
Dababiya (GSSP)
Circum-Caribbean Volcanism
Paleocene/Eocene Boundary (55.8 Ma): P/E Thermal Maximum (PETM)

Figure 2

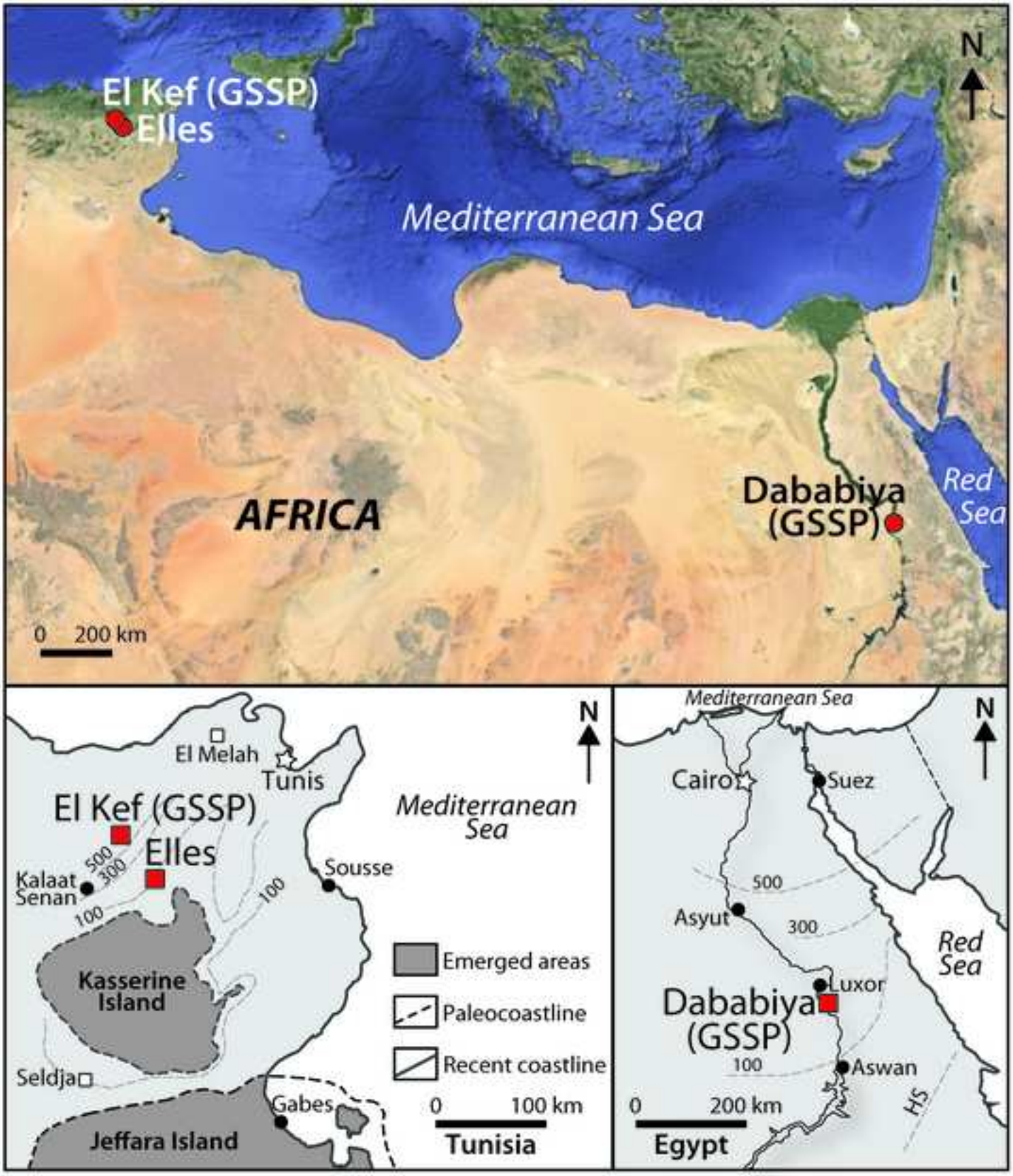
El Kef (GSSP)
Elles
Mediterranean Sea
N
AFRICA
Dababiya
(GSSP)
Red
Sea
0 200 km
El Melah
Tunis
El Kef (GSSP)
Elles
Mediterranean
Sea
Kalaat
Senan
500
300
100
100
Sousse
Kasserine
Island
Seldja
Gabes
Jeffara Island
Emerged areas
Paleocoastline
Recent coastline
0 100 km
Tunisia
Mediterranean Sea
Cairo
Suez
500
Asyut
300
Red
Sea
Luxor
Dababiya
(GSSP)
100
Aswan
HS
0 200 km
Egypt

Figure 3

Figure 4

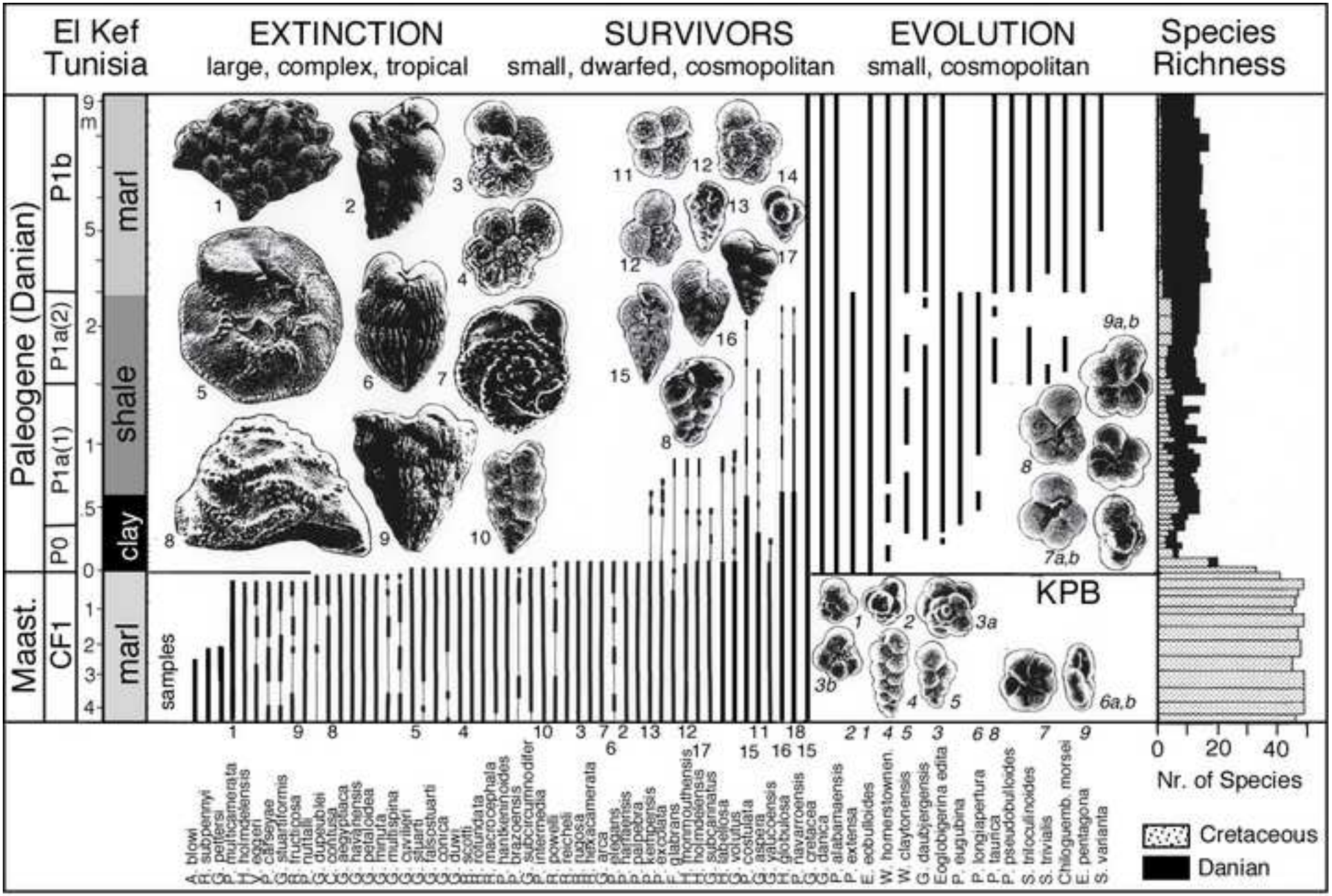
El Kef
Tunisia
EXTINCTION
large, complex, tropical
SURVIVORS
small, dwarfed, cosmopolitan
EVOLUTION
small, cosmopolitan
Species
Richness
Paleogene (Danian)
Maast.
P1b
P1a(2)
P1a(1)
P0
CF1
marl
shale
clay
marl
m
samples
KPB
Nr. of Species
0
20
40
Cretaceous
Danian
A. blowi
A. subpenmyi
P. pelfersi
M. multicamerata
M. holmdelensis
M. eggeri
M. carseyae
M. stuartiformis
M. fructicosa
M. nuttalli
M. dupeubki
M. conflusa
M. aegyptiaca
M. havanensis
M. petaloidea
M. hirsuta
M. multispina
M. cerroliqri
M. stuarti
M. falsostuarti
M. conica
M. duwi
M. scotti
M. rotundata
M. macrocephala
M. hantkeninoides
M. brazoensis
M. subcircumnodifer
M. intermedia
M. powelli
M. reicheli
M. rugosa
M. hexacamerata
M. arca
M. elegans
M. haraensis
M. palpebra
M. kempensis
M. exocolata
M. glabrans
M. monmouthensis
M. holmdeensis
M. subcarinatus
M. labelliosa
M. volutus
M. costulata
M. aspera
M. yaucoensis
M. globulosa
M. navarroensis
P. cretacea
P. danica
P. alabamaensis
P. extensa
E. eobulloides
W. homerstownen.
W. claytonensis
G. dautjergensis
Eoglobigerina edita
P. eugubina
P. longiapertura
P. taunica
P. pseudobulloides
S. triloculinoides
S. trivialis
Chiloguemb. morsei
E. pentagona
S. varianta

Figure 5

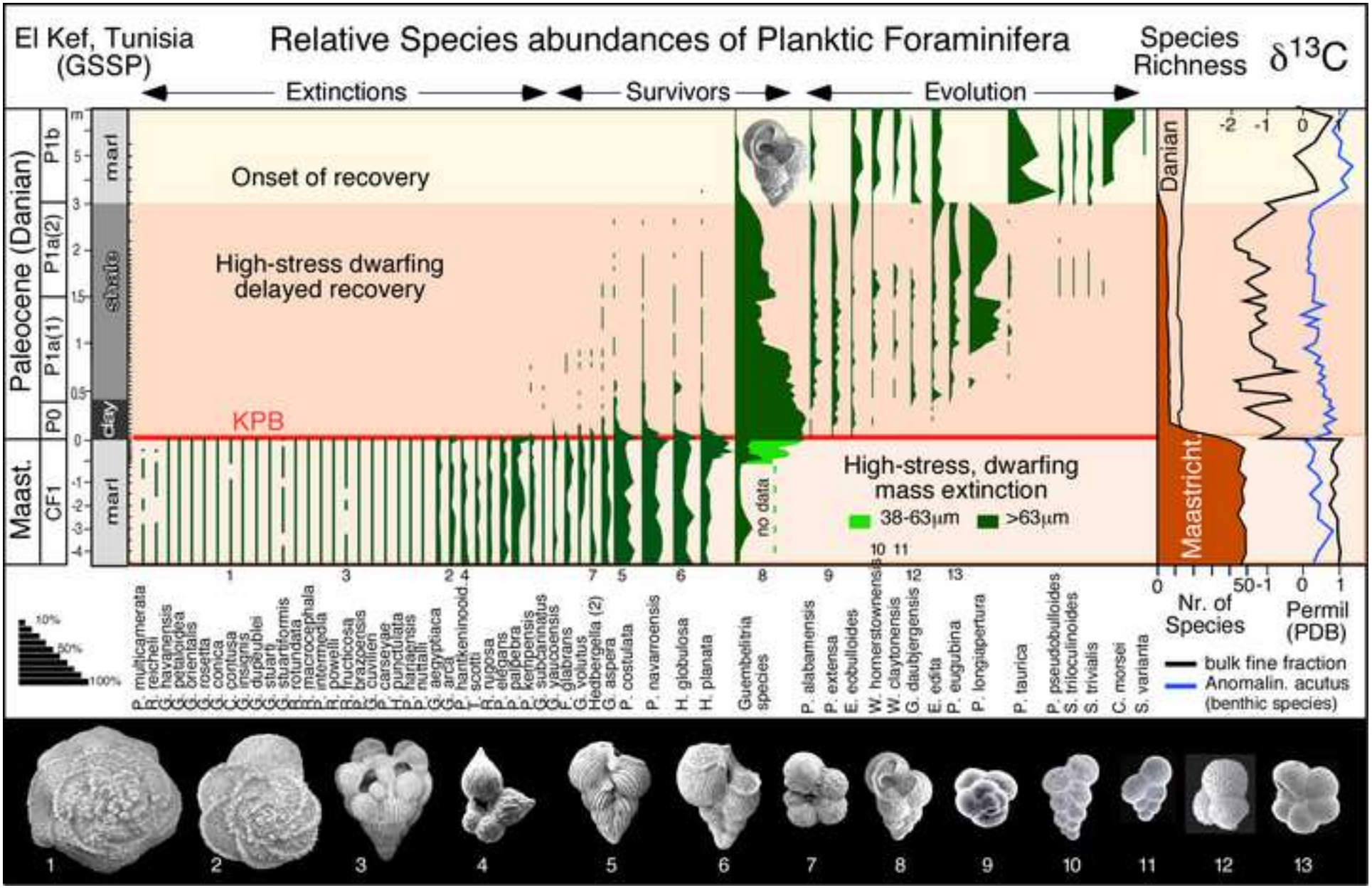
El Kef, Tunisia (GSSP)
Relative Species abundances of Planktic Foraminifera
Species Richness
δ13C
Extinctions
Survivors
Evolution
Paleocene (Danian)
Maast.
P1b
P1a(2)
P1a(1)
P0
CF1
marl
shale
clay
marl
Onset of recovery
High-stress dwarfing delayed recovery
KPB
High-stress, dwarfing mass extinction
38-63µm
>63µm
no data
Danian
Maastricht.
Nr. of Species
Permil (PDB)
bulk fine fraction
Anomalin. acutus (benthic species)
P. multicamerata
R. reicheli
H. havanensis
G. petaloidea
G. orientalis
R. rosetta
R. conica
R. contusa
R. insignis
R. duplebulei
R. stuarti
R. stuartiformis
R. rotundata
R. macrocephala
R. intermedia
R. powelli
R. fructicosa
R. brazoensis
R. cuvillieri
R. carseyae
R. punctulata
R. hariaensis
R. nuttalli
R. aegyptiaca
R. arca
R. hantkeninoid.
R. scotti
R. ruposa
R. elegans
R. palpebra
P. kempensis
P. subcarinatus
G. yaucoensis
P. glabrans
G. volutus
Hedbergella (2)
G. aspera
P. costulata
P. navarroensis
H. globulosa
H. planata
Guembelitria species
P. alabamensis
P. extensa
E. eobulloides
W. homerstownensis
W. claytonensis
G. daubjergensis
E. edita
P. eugubina
P. longiapertura
P. taurica
P. pseudobulloides
S. trilociculinoides
S. trivialis
C. morsei
S. varianta
10%
50%
100%
1
2
3
4
5
6
7
8
9
10
11
12
13

Figure 6

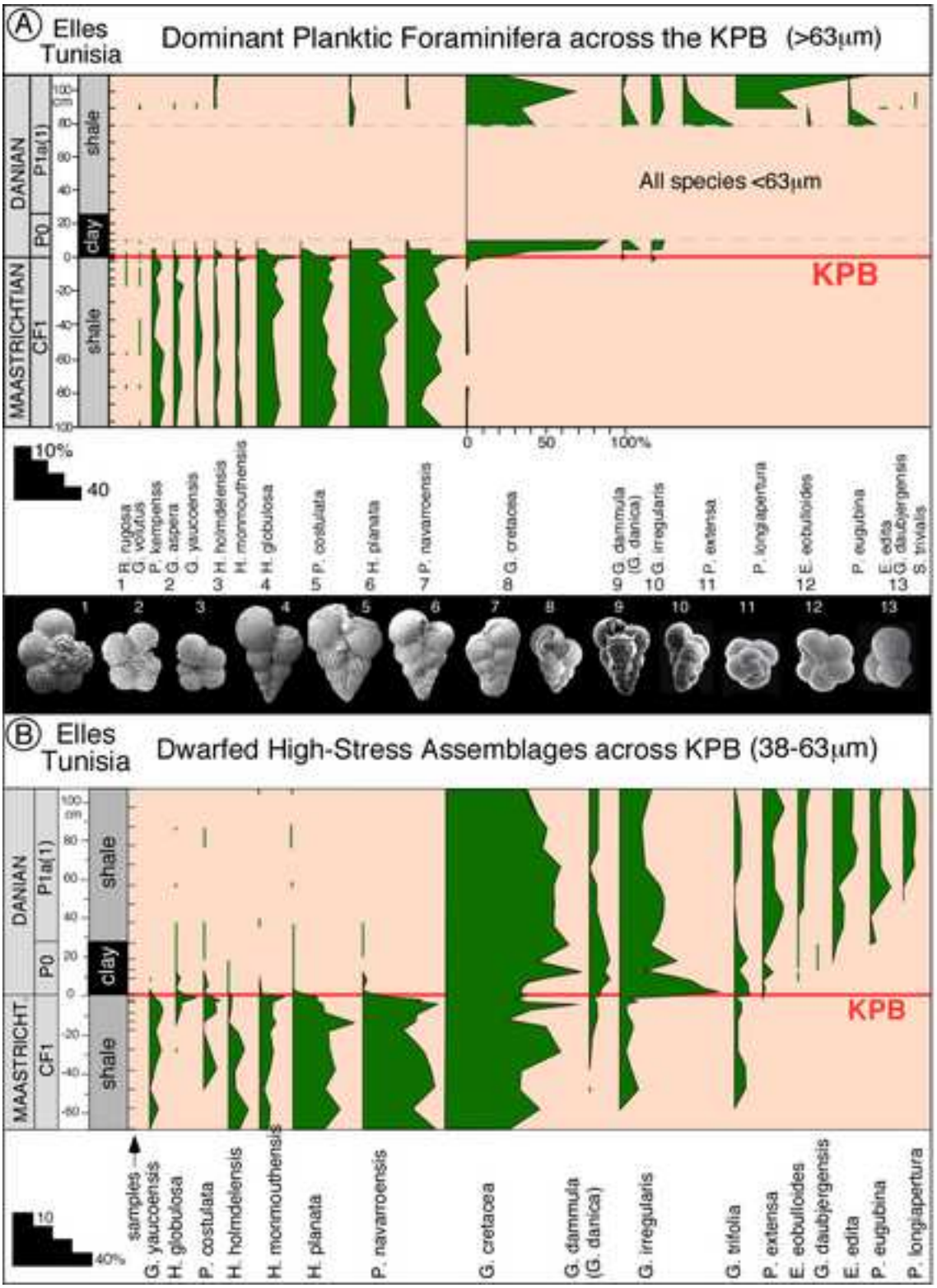
A
Elles
Tunisia
Dominant Planktic Foraminifera across the KPB (>63µm)
DANIAN
P1a(1)
P0
MAASTRICHTIAN
CF1
shale
clay
shale
All species <63µm
KPB
0
50
100%
10%
40
R. rugosa
G. voltuis
P. kempensis
G. aspera
G. yaucoensis
H. holmdelensis
H. monmouthensis
H. globulosa
P. costulata
H. planata
P. navarroensis
G. cretacea
G. dammula (G. danica)
G. irregularis
P. extensa
P. longiapertura
E. eobulloides
P. eugubina
E. edita
G. daubjergensis
S. trivialis
1
2
3
4
5
6
7
8
9
10
11
12
13
B
Elles
Tunisia
Dwarfed High-Stress Assemblages across KPB (38-63µm)
DANIAN
P1a(1)
P0
MAASTRICHT
CF1
shale
clay
shale
KPB
10
40%
samples
G. yaucoensis
H. globulosa
P. costulata
H. holmdelensis
H. monmouthensis
H. planata
P. navarroensis
G. cretacea
G. dammula (G. danica)
G. irregularis
G. trifolia
P. extensa
E. eobulloides
G. daubjergensis
E. edita
P. eugubina
P. longiapertura

Figure 7

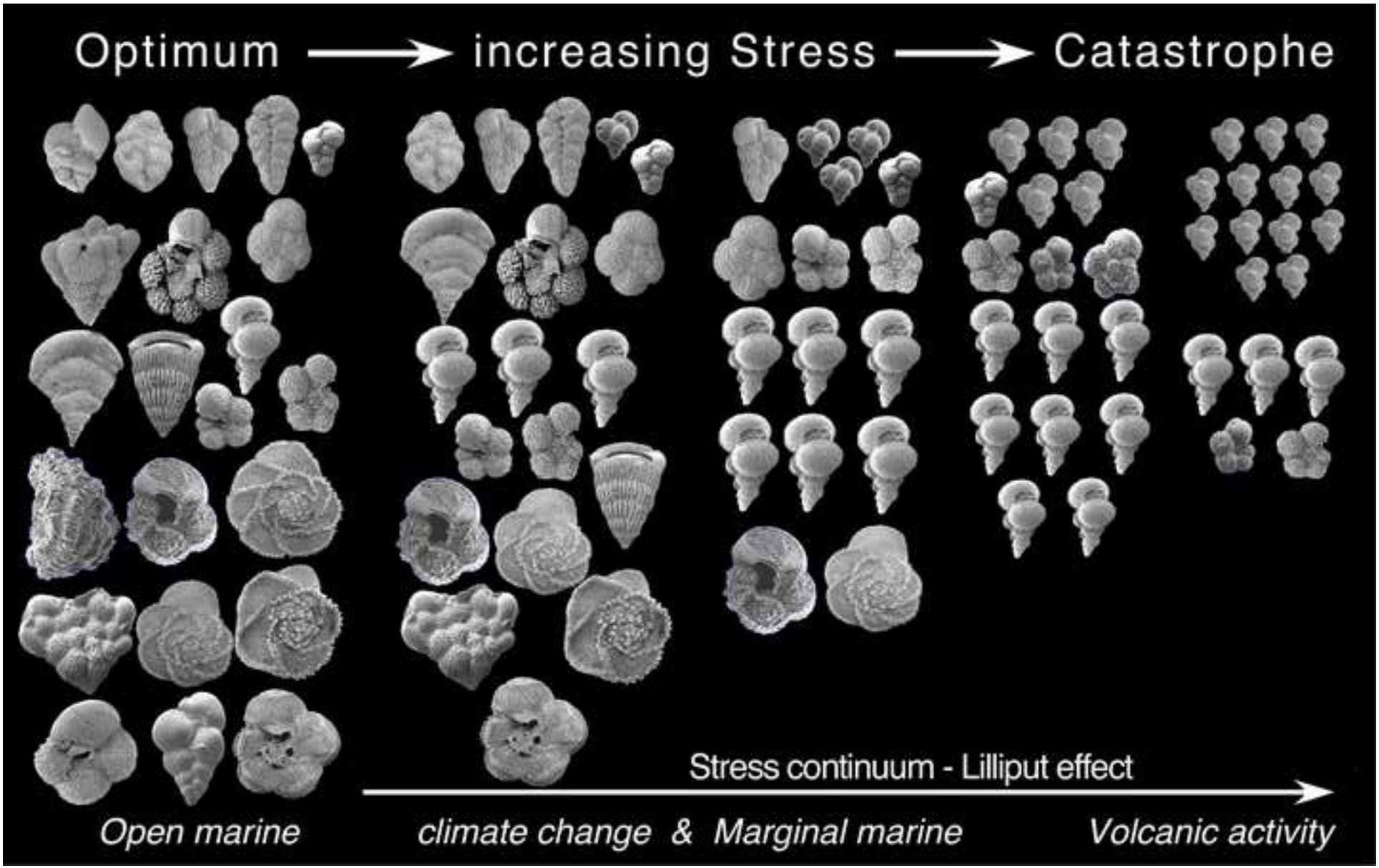
Optimum
increasing Stress
Catastrophe
Stress continuum - Lilliput effect
Open marine
climate change & Marginal marine
Volcanic activity

Figure 8

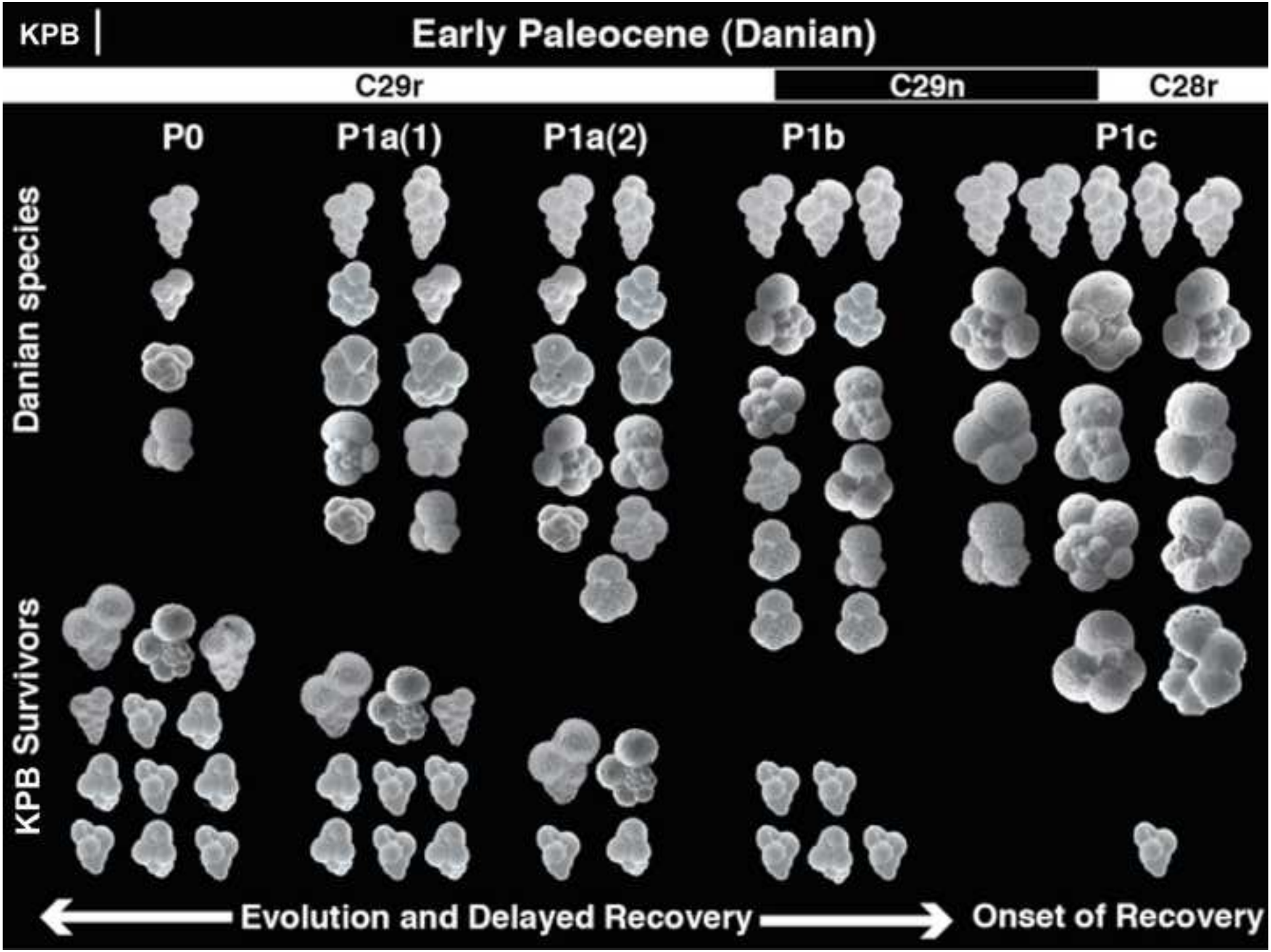
KPB
Early Paleocene (Danian)
C29r
C29n
C28r
P0
P1a(1)
P1a(2)
P1b
P1c
Danian species
KPB Survivors
Evolution and Delayed Recovery
Onset of Recovery

Figure 9

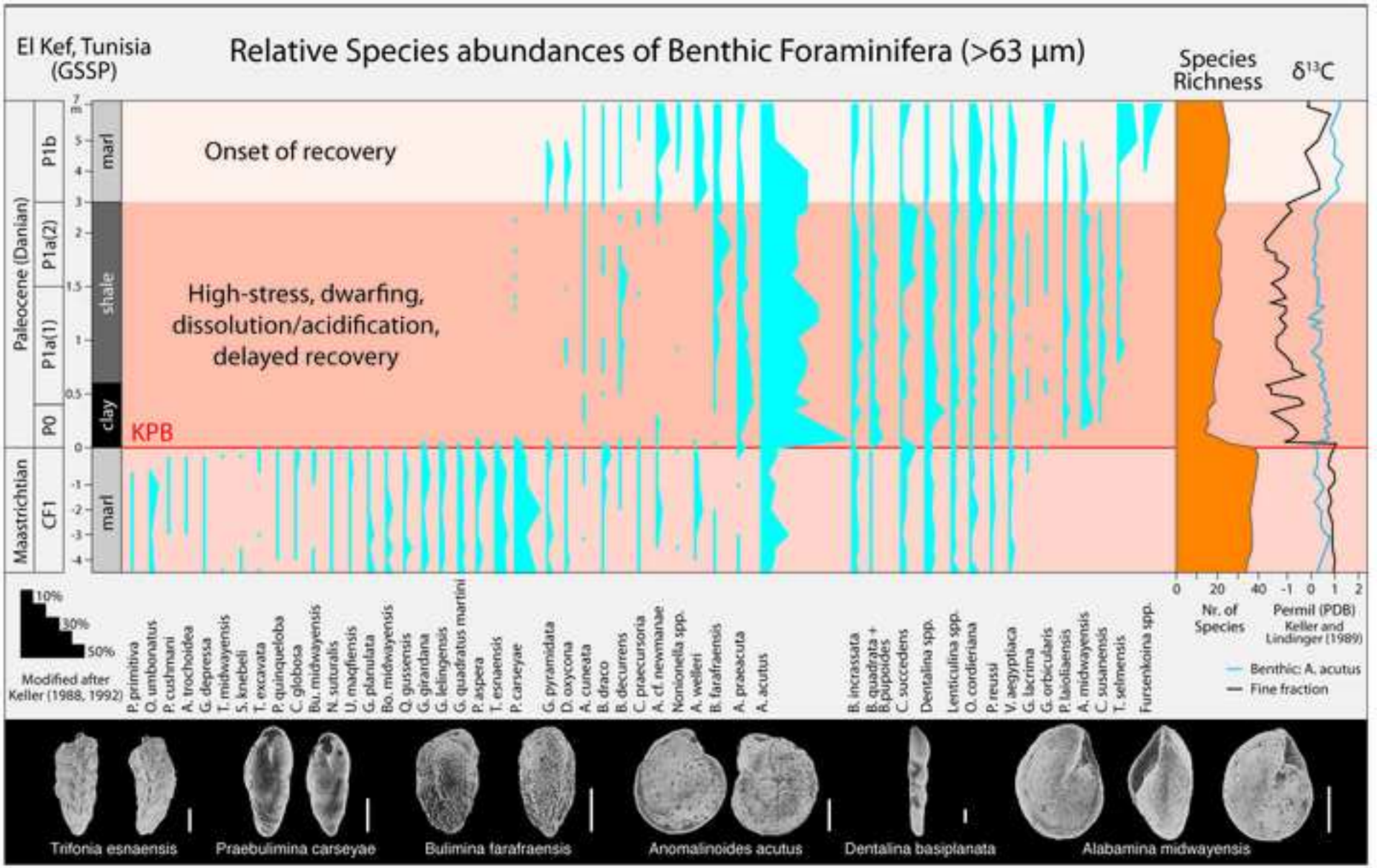
El Kef, Tunisia
(GSSP)
Relative Species abundances of Benthic Foraminifera (>63 µm)
Species Richness
δ13C
Paleocene (Danian)
Maastrichtian
P1b
P1a(2)
P1a(1)
P0
CF1
marl
shale
clay
marl
Onset of recovery
High-stress, dwarfing, dissolution/acidification, delayed recovery
KPB
10%
30%
50%
Modified after Keller (1988, 1992)
P. primitiva
O. umbonatus
P. cushmani
A. trochoidea
G. depressa
T. midwayensis
S. knebeli
T. excavata
P. quinqueloba
C. globosa
Bu. midwayensis
N. suturalis
U. maqfiensis
G. planulata
Bo. midwayensis
Q. gussensis
G. girardana
G. lelingensis
G. quadratus martini
P. aspera
T. esnaensis
P. carseyae
G. pyramidata
D. oxycona
A. cuneata
B. draco
B. decurrens
C. praecursoria
A. cf. newmanae
Nonionella spp.
A. wellieri
B. farafraensis
A. praeacuta
A. acutus
B. incrassata
B. quadrata + B.pupoides
C. succedens
Dentalina spp.
Lenticulina spp.
O. cordieriana
P. reussi
V. aegyptiaca
G. lacrima
G. orbiculatis
P. laioliaensis
A. midwayensis
C. susanensis
T. selimensis
Fursenkoina spp.
0
20
40
Nr. of Species
-1
0
1
2
Permil (PDB) Keller and Lindinger (1989)
Benthic: A. acutus
Fine fraction
Trifonia esnaensis
Praebulimina carseyae
Bulimina farafraensis
Anomalinoides acutus
Dentalina basiplanata
Alabamina midwayensis

Figure 10

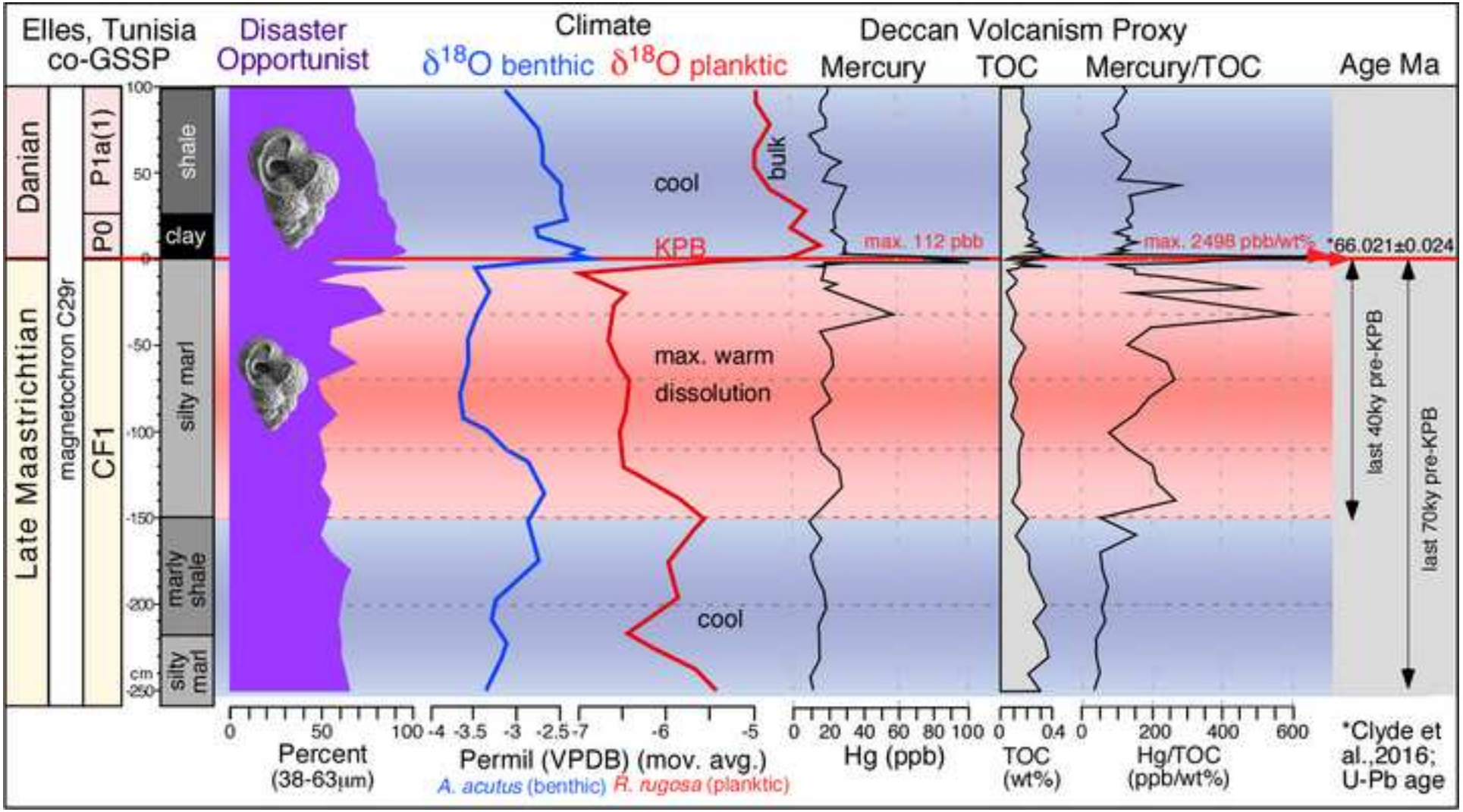
Elles, Tunisia
co-GSSP
Disaster
Opportunist
Climate
δ18O benthic
δ18O planktic
Deccan Volcanism Proxy
Mercury
TOC
Mercury/TOC
Age Ma
Danian
Late Maastrichtian
magnetochron C29r
P1a(1)
P0
CF1
shale
clay
silty marl
marly shale
silty marl
cm
cool
bulk
KPB
max. 112 pbb
max. 2498 pbb/wt%
*66.021±0.024
max. warm
dissolution
cool
last 40ky pre-KPB
last 70ky pre-KPB
Percent
(38-63μm)
Permil (VPDB) (mov. avg.)
A. acutus (benthic) R. rugosa (planktic)
Hg (ppb)
TOC
(wt%)
Hg/TOC
(ppb/wt%)
*Clyde et
al.,2016;
U-Pb age

Figure 11

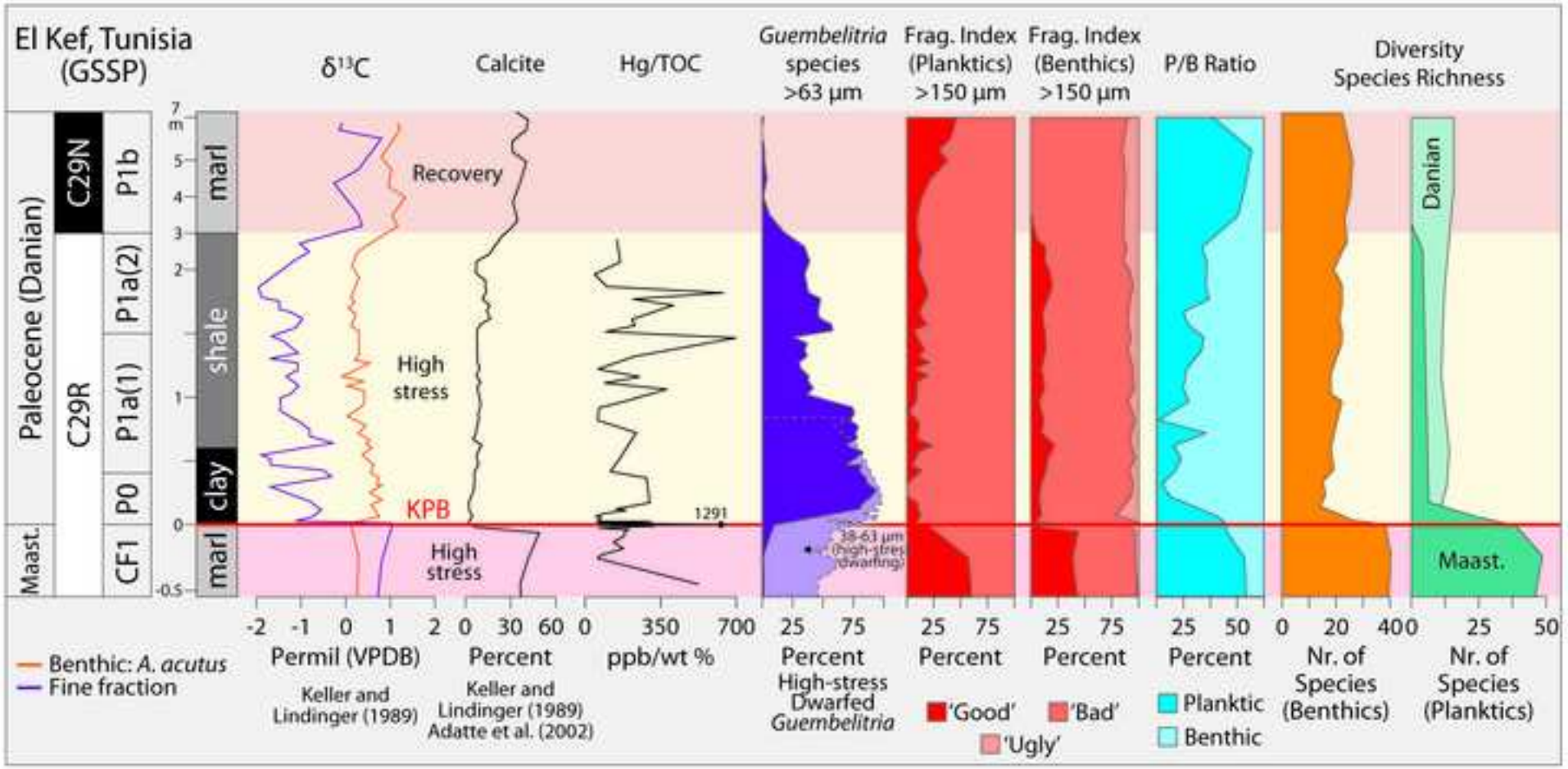
El Kef, Tunisia
(GSSP)
δ13C
Calcite
Hg/TOC
Guembelitria species >63 µm
Frag. Index (Planktics) >150 µm
Frag. Index (Benthics) >150 µm
P/B Ratio
Diversity Species Richness
Paleocene (Danian)
Maast.
C29N
C29R
P1b
P1a(2)
P1a(1)
P0
CF1
marl
shale
clay
marl
7 m
5
4
3
2
1
0
-0.5
Recovery
High stress
KPB
High stress
1291
38-63 µm (high-stress dwarfing)
Danian
Maast.
-2 -1 0 1 2
Permil (VPDB)
Keller and Lindinger (1989)
0 30 60
Percent
Keller and Lindinger (1989) Adatte et al. (2002)
0 350 700
ppb/wt %
25 75
Percent
High-stress Dwarfed Guembelitria
25 75
Percent
'Good'
'Ugly'
25 75
Percent
'Bad'
25 50
Percent
Planktic
Benthic
0 20 40
Nr. of Species (Benthics)
0 25 50
Nr. of Species (Planktics)
Benthic: A. acutus
Fine fraction

Figure 12


A
GSSP
sampled
East 25m
GSSP
B
C
Esna-2
Esna-1
PALEOCENE
EOCENE
PEB
East 25m
GSSP
PETM-CIE
PALEOCENE
EOCENE

Figure 13

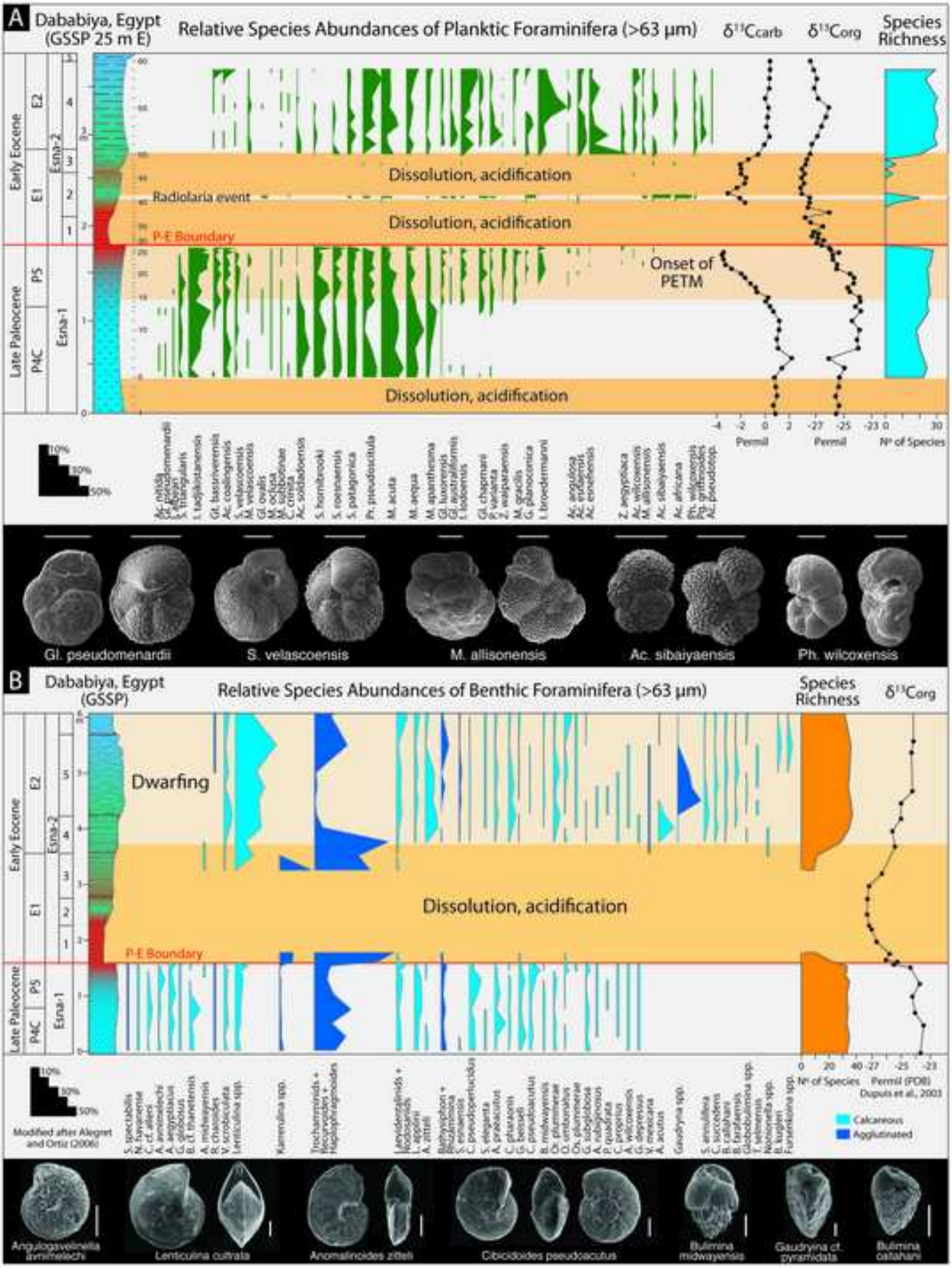
A
Dababiya, Egypt
(GSSP 25 m E)
Relative Species Abundances of Planktic Foraminifera (>63 µm)
δ13Ccarb
δ13Corg
Species Richness
Early Eocene
Late Paleocene
E2
E1
P5
P4C
Esna-2
Esna-1
Dissolution, acidification
Radiolaria event
Dissolution, acidification
P-E Boundary
Onset of PETM
Dissolution, acidification
Permil
Permil
Nº of Species
Gl. pseudomenardii
S. velascoensis
M. allisonensis
Ac. sibaiyaensis
Ph. wilcoxensis
B
Dababiya, Egypt
(GSSP)
Relative Species Abundances of Benthic Foraminifera (>63 µm)
Species Richness
δ13Corg
Dwarfing
Dissolution, acidification
P-E Boundary
Nº of Species
Permil (PDB)
Dupuis et al., 2003
Calcareous
Agglutinated
Modified after Alegret and Ortiz (2006)
Angulogavelinella avnimelechi
Lenticulina cultrata
Anomalinoides zitteli
Cibicidoides pseudoacutus
Bulimina midwayensis
Gaudryina cf. pyramidata
Bulimina callahani

Figure 14

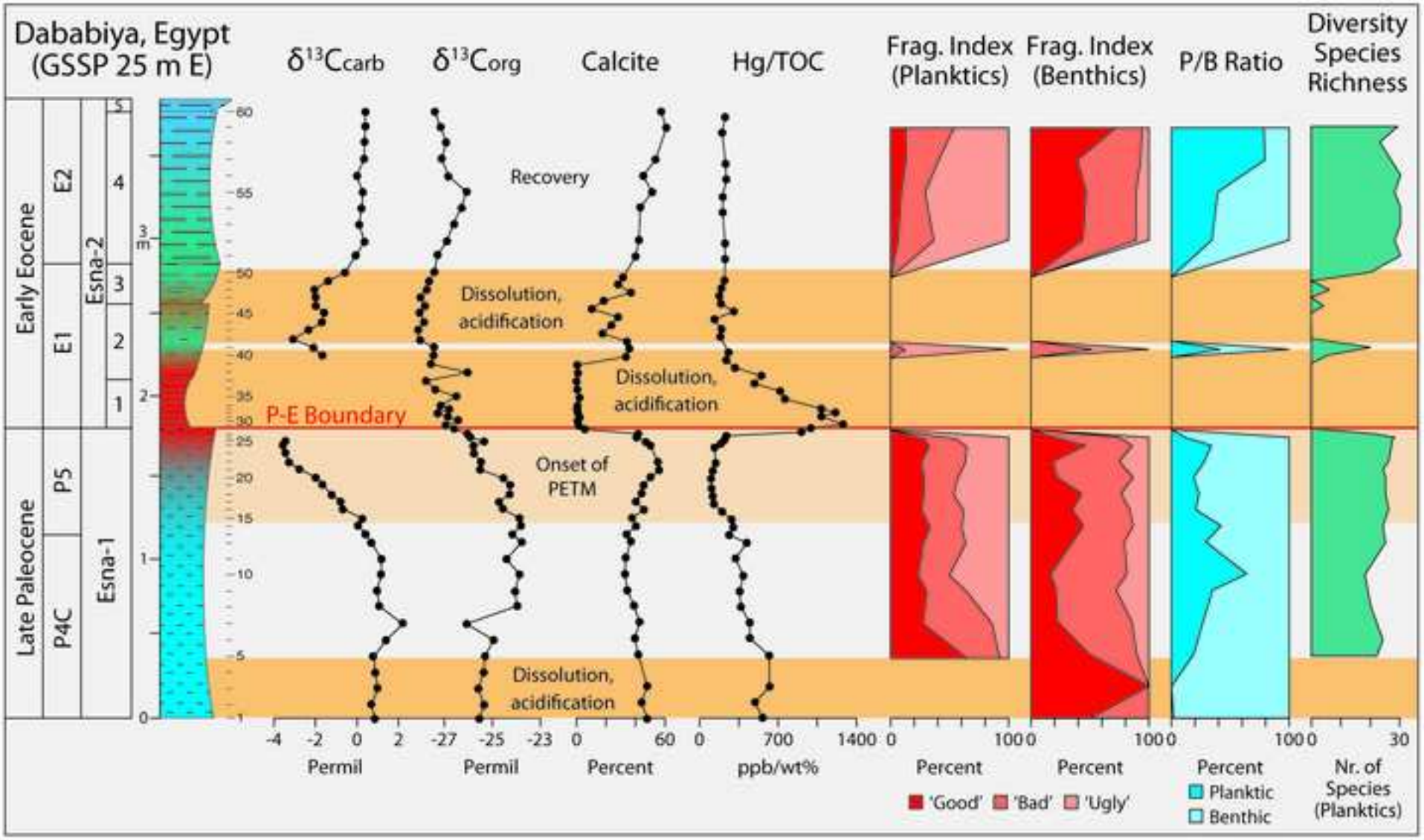
Dababiya, Egypt
(GSSP 25 m E)
δ13Ccarb
δ13Corg
Calcite
Hg/TOC
Frag. Index (Planktics)
Frag. Index (Benthics)
P/B Ratio
Diversity Species Richness
Early Eocene
Late Paleocene
E2
E1
P5
P4C
Esna-2
Esna-1
Recovery
Dissolution, acidification
Dissolution, acidification
P-E Boundary
Onset of PETM
Dissolution, acidification
Permil
Permil
Percent
ppb/wt%
Percent
Percent
Percent
Nr. of Species (Planktics)
'Good'
'Bad'
'Ugly'
Planktic
Benthic

Figure 15

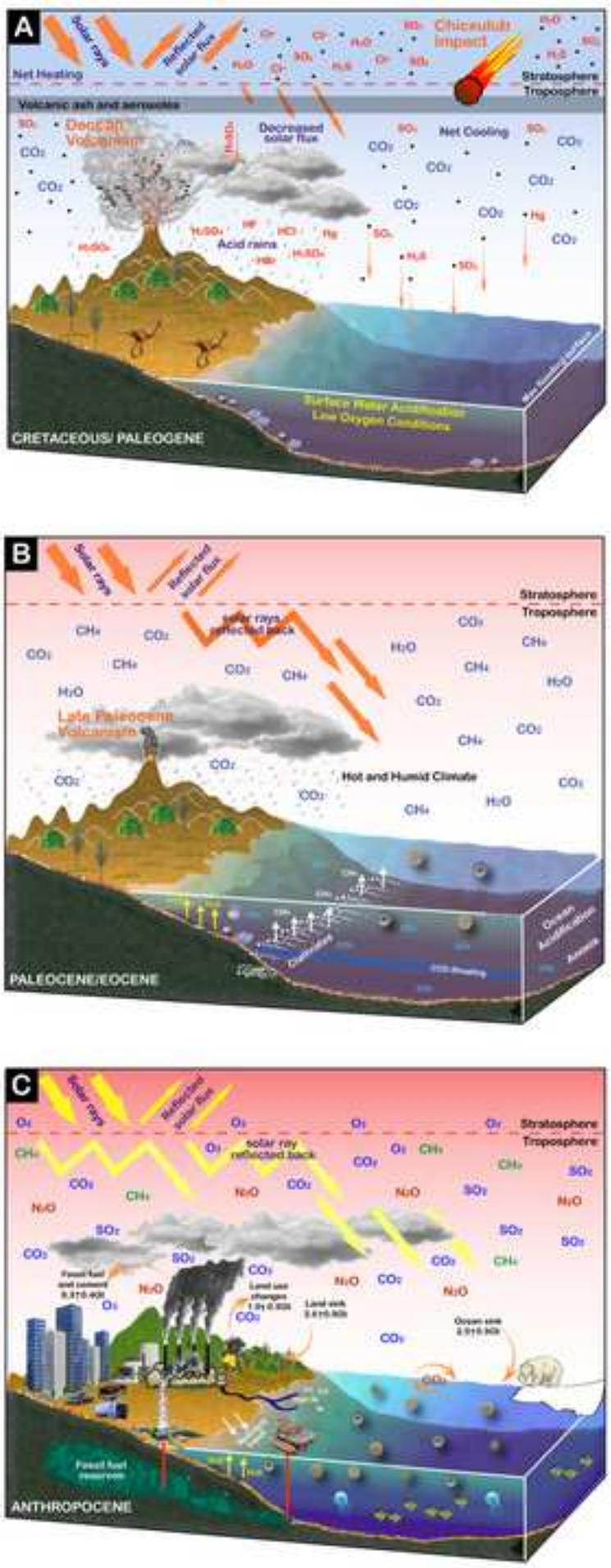
A
Solar rays
Reflected solar flux
Net Heating
Chicxulub Impact
Stratosphere
Troposphere
Volcanic ash and aerosoles
Deccan Volcanism
Decreased solar flux
Net Cooling
Acid rains
Surface Water Acidification
Low Oxygen Conditions
CRETACEOUS/ PALEOCENE
B
Solar rays
Reflected solar flux
Stratosphere
Troposphere
solar rays reflected back
Late Paleocene Volcanism
Hot and Humid Climate
Ocean Acidification
PALEOCENE/EOCENE
C
Solar rays
Reflected solar flux
Stratosphere
Troposphere
solar ray reflected back
ANTHROPOCENE

Table 1

Events	Anthropocene: Mass Extinction?	Paleocene/Eocene: PETM	End-Cretaceous: Mass Extinction
Age (Ma)	Ongoing, predicted by ~2250-2500[1]	55.8±0.2 Ma	66.021±0.024 Ma
Faunal turnover	Ongoing extinctions	Extinctions/originations	Mass extinction
Mass extinctions	In progress	Minor[2]	~50% genera, ~75% species
Rate of extinctions	In accelerating phase 20-50X background rates[1]	Rapid at max. warming 6-12X background rates in benthic foraminifera[2]	Rapid over ~1000 years ~220X background rate in planktic foraminifera[3]
Benthic foram extinctions	Yes, ongoing	30-50% species	Minor
Planktic foram extinctions	Yes, ongoing	Minor	99% species
Vertebrate extinctions	Yes, ongoing	Minor, migration	Major
Terrestrial extinctions	Yes, ongoing	Minor	Major
Recovery	----------	Rapid after PETM	Delayed >500 ky
Pre-event climate	Gradual warming	Gradual warming	Rapid warm-cool changes over 350 ky[4]
Climate (greenhouse gases)	Rapid warming	Rapid warming	Rapid warming
Warming: rate	1-4 °C/100 yrs, 2-10 °C next 200-300 yrs	0.025 °C/100 yrs, total 5 °C[5]	Oceans 3-4 °C[4] Land 6-8 °C[6]
Warming: max duration	Decades to 100's of years	Tens of thousands of years	Tens of thousands of years
Tipping point temperature increase >4°C	~4 °C possibly reached by 2020	5 °C	~5 °C
Sea-level	Rapid rise (1-2 m)[7]	Rapid rise (3-5 m)	Rise ~50 m over 100 ky
Anoxia/ dysoxia	Yes	Yes, continental shelf	Dysoxia in water column
Ocean Acidification (rate)	Yes (0.3 units/100 yrs)[8]	Yes (0.3 units/20 ky)[9]	Yes[10]
Clathrates (CH_4)	No (possible in future)	Yes	None confirmed
Volcanism (LIPs)	No	North Atlantic Igneous Province (NAIP)	Deccan Traps
Global warming: main underlying cause(s)	CO_2: fossil fuel burning CH_4: peat, coal, permafrost	CO_2: volcanoes, CH_4: clathrates, peat, coal, permafrost	CO_2: volcanoes CH_4: no data
Impacts	No	Unconfirmed	Chicxulub 180 km

[1] Anthropocene extinctions are predicted to reach the 75 % mass extinction level within the next 250 to 500 ky (conservative estimate) based on projection of current rates of extinctions and current rates of fossil fuel burning (e.g. May et al., 1995; Hughes et al., 1997; Ceballos and Ehrlich, 2002; Pereira et al., 2010; Barnosky et al., 2011).

[2] For the PETM event extinctions are limited to benthic foraminifera in the marine realm; with maximum 50 % extinct over 170 ky (estimated duration of PETM event), the rate of extinction estimated from El Kef is 0.12 species/ky or about 12-24 background rates at 1-2 species/100 ky (this study).

[3] Estimated from planktic foraminifera: 66 % (44 species) extinct over about 10 ky, an average of 4.4 species/ky; background rates are 1-2 species/100 ky or 0.01-0.02/ky. This means that the rate of extinction is at least 220 times background. About 33 % go extinct within 50-100 ky after the KPB leaving a single survivor species (this study).

[4] e.g., Stüben et al. (2003), Li and Keller (1998), Abramovich and Keller (2003), Punekar et al. (2014)

[5] Zachos et al. (2005, 2006)

[6] Wilf et al. (2003), Nordt et al. (2003)

[7] IPCC 5th Assessment Report (2013), conservative estimate

[8] e.g., Sluijs et al. (2008), IPCC 4th Assessment Report (2007), projected global average pH surface ocean, between 2000-2100

[9] Penman et al. (2014), comparison of $\delta^{11}B$ data and LOSCAR model simulation

[10] Font et al. (2011, 2014), Punekar et al. (2016)